

A DISSERTATION ON

DESIGN AND IMPLEMENTATION OF L BAND

MICROSTRIP COUPLER WITH IMPROVED COUPLING

AND HIGH DIRECTIVITY

Submitted towards the Partial Fulfilment of the Requirement for the
award of the degree of

Master of Technology
in
Microwave & Optical Communication

Submitted by
Harish Chandra Kumawat
2K12/MOC/07

Under the supervision of
Dr. Priyanka Jain
(Assistant Professor)
Department of Electronics & Communication Engineering



DEPARTMENT OF ELECTRONICS & COMMUNICATION AND
APPLIED PHYSICS

DELHI TECHNOLOGICAL UNIVERSITY

NEW DELHI-110042

JULY 2014



DELHI TECHNOLOGICAL UNIVERSITY
(Formerly Delhi College of Engineering)
SHAHBAD DAULATPUR, BAWANA ROAD,
DELHI- 110042

CERTIFICATE

This is to certify that the dissertation title “**Design and Implementation of L Band Microstrip Coupler with improved Coupling and High Directivity** ” is the authentic work of **Mr. Harish Chandra Kumawat** under my guidance and supervision in the partial fulfilment of requirement towards the degree of Master of Technology in **Microwave and Optical Communication**, jointly run by the Department of Electronics and Communication Engineering and Department of Applied Physics at **Delhi Technological University, New Delhi**. To the best of my knowledge, the matter embodied in the thesis has not been submitted to any other University/ Institute for the award of any other degree.

Dr. Priyanka Jain

Supervisor

Assistant Professor (ECE)

Delhi Technological University

Prof. Rajiv Kapoor

Head of Department

Department of ECE

Delhi Technological University

DECLARATION

I hereby declare that all the information in these documents has been obtained and presented in accordance with academic rules and ethical conduct. It is being submitted for the degree of Master of Technology in Microwave and Optical Communication at Delhi Technological University. It has not been submitted before for any degree or examination in any other university.

Harish Chandra Kumawat

Date:

ACKNOWLEDGEMENT

With all praises to the almighty and by His blessings I have finally completed this thesis.

I would like to express my gratitude to **Dr. Priyanka Jain**, Assistant Professor, Department of Electronics & Communication Engineering, Delhi Technological University, New Delhi, who has graciously provided me her valuable time whenever I required her assistance. Her counselling, supervision and suggestions were always encouraging and it motivated me to complete the job at hand. She will always be regarded as a great mentor for me.

I am deeply grateful to **Prof. Rajiv Kapoor**, Head of Department (Electronics and Communication Engineering), Delhi Technological University for his support and encouragement in carrying out this project.

I would like to express my heartiest thank to my friends, seniors and juniors for constant support and motivation. Last but not least I thank my parents, for everything I am and will be in future. It's your unspoken prayers and affection that keep me moving forward.

Harish Chandra Kumawat
M.Tech. (MOC)
2K12/MOC/07

ABSTRACT

The couplers are passive devices used in the field of radio technology. They couple a defined amount of the electromagnetic power in a transmission line to a port enabling the signal to be used in another circuit. Directional couplers are most frequently constructed from two coupled transmission lines set close enough together such that energy passing through one is coupled to the other.

In this thesis work, a new symmetrical coupled-line circuit structure without any patterned ground plane is proposed to design tight-coupling high-directivity couplers for L Band, which would be found in numerous applications in a microstrip RF front end because of its simple structure and inherent excellent compatibility.

Based on a traditional even- and odd-mode technique, closed-form mathematical equations for both circuit electrical parameters and scattering parameters are obtained. Due to the use of two coupled-line sections placed in the vertical direction, the directivity of this novel coupler without any other compensation techniques can be enhanced while maintaining tight-coupling.

This microstrip coupled-line coupler can be used for the designs of various balanced power amplifiers, mixers, modulators, measurement systems, circularly polarized antennas, beam-forming array antennas, etc.

Advanced Design System (ADS) tool was used for design and simulation. The simulated results show good return loss, quadrature phase characteristics, high directivity, and strong coupling performances of the coupler.

TABLE OF CONTENTS

CERTIFICATE	ii
DECLARATION	iii
ACKNOWLEDGMENT	iv
ABSTRACT	v
TABLE OF CONTENTS	vi
LIST OF FIGURES	viii
LIST OF TABLES	x
LIST OF SYMBOLS	xi
LIST OF ABBREVIATIONS	xiv
CHAPTER 1: INTRODUCTION	1
1.1 Motivation	2
1.2 Research Objectives	2
1.3 Thesis Organization	3
CHAPTER 2: LITERATURE REVIEW	5
2.1 Definition of Coupler	5
2.2 Literature Survey	6
CHAPTER 3: BASIC PROPERTIES OF DIRECTIONAL COUPLER	9
3.1 Four Port Networks	9
3.2 Directional Couplers Characterization	11
3.2.1 Coupling C	12
3.2.2 Isolation I	12
3.2.3 Directivity D	13
3.2.4 Insertion Loss	13

CHAPTER 4: COUPLED-LINE COUPLER AND ITS DESIGN THEORY	15
4.1 Microstrip Line	15
4.2 Coupled Line	16
4.2.1 Couples Line Theory	16
4.3 Design Calculation for Proposed Coupler	19
4.4 Analysis of Circuit Electrical Parameters and Scattering Parameters	32
CHAPTER 5: SIMULATION AND SIMULATED RESULT	37
5.1 What is Advanced Design System (ADS)?	37
5.2 Full Wave Simulation of Coupler	37
5.3 Result	44
CHAPTER 6: CONCLUSION AND FUTURE WORK	46
6.1 Conclusion	46
6.2 Future Work	47
REFERENCES	48
APPEDDIX	51

LIST OF FIGURE

Figure No.	Description	Page No.
2.1	Commonly used symbols for directional couplers, and power flow conventions	5
3.1	Basic block diagram of Direction Coupler	11
4.1	Microstrip transmission line	15
4.2	Various coupled transmission line geometries	16
4.3	A three-wire coupled transmission line and its equivalent capacitance network	17
4.4	Even- and odd-mode excitations for a coupled line, and the resulting equivalent capacitance networks	17
4.5	Circuit Schematic of the proposed Coupler	19
4.6	Even-even mode excitation	19
4.7	Even-Odd Mode excitation	20
4.8	Odd-Even Mode excitation	20
4.9	Odd-Odd Mode excitation	21
4.10	Even-Even Mode	24
4.11	Even-Odd Mode	25
4.12	Odd-Even Mode	25
4.13	Odd-Odd Mode	26
4.14	Calculated Parameters z_{e2} and z_{o2} with different values of θ_2	33
4.15	Calculated Coupling Coefficient with different values of θ_2	33
4.16	Scattering parameters and Phase difference of the coupler with electrical length $\theta_2=40^\circ$ and 50°	34
4.17	Calculated Parameters z_{e2} and z_{o2} with different values of θ_1	35
4.18	Calculated Coupling Coefficient with different values of θ_1	35

4.19	Scattering parameters and Phase difference of the coupler with electrical length $\theta_1=50^\circ$ and 60°	36
5.1	ADS Line Calculator	38
5.2	Layout of the coupler	39
5.3	Full wave simulated Scattering parameters of Coupler without optimization	40
5.4	Coupler Layout Design in ADS Software	41
5.5	Scattering Parameter S11	41
5.6	Scattering Parameter S21	42
5.7	Scattering Parameter S31	42
5.8	Scattering Parameter S41	43
5.9	Full wave simulated Scattering parameters of Coupler	43
5.10	Phase difference between S21 and S31	44

LIST OF TABLES

Table No.	Description	Page No.
3.1	Coupling Insertion Loss	14

LIST OF SYMBOLS

S	Scattering Parameter
[S]	Scattering matrix
E	Electric field
H	Magnetic field
P_1	Input power at port 1
P_2	Power at port 2
P_3	Output power at port 3
P_4	Output power at port 4
C	Coupling
I	Isolation
D	Directivity
IL	Insertion Loss
ϵ_r	Dielectric constant
Z_{0e}	Even mode characteristic impedance
Z_{0o}	Odd mode characteristic impedance
V	Voltage
V_1^+	Input Voltage at port 1
V_2^+	Input Voltage at port 2
V_3^+	Input Voltage at port 3
V_4^+	Input Voltage at port 4

V_1^-	Reflected Voltage at port 1
V_2^-	Reflected Voltage at port 2
V_3^-	Reflected Voltage at port 3
V_4^-	Reflected Voltage at port 4
Γ	Reflection Coefficient
Γ_{ee}	Reflection Coefficient for even even mode
Γ_{eo}	Reflection Coefficient for even odd mode
Γ_{oe}	Reflection Coefficient for odd even mode
Γ_{oo}	Reflection Coefficient for odd odd mode
Z	Impedance
Z_o	Port impedance
Z_{inee}	Input impedance for even even mode
Z_{ineo}	Input impedance for even odd mode
Z_{inoe}	Input impedance for odd even mode
Z_{inoo}	Input impedance for odd odd mode
Z_{e1}	Normalized characteristic impedance of first coupled line in even mode
Z_{o1}	Normalized characteristic impedance of first coupled line in odd mode
Z_{e2}	Normalized characteristic impedance of second coupled line in even mode
Z_{o2}	Normalized characteristic impedance of second coupled line in odd mode
Θ	Electrical Length
θ_{e1}	Electrical length of first coupled line in even mode
θ_{o1}	Electrical length of first coupled line in odd mode
θ_{e2}	Electrical length of second coupled line in even mode

θ_{o2} Electrical length of second coupled line in odd mode

K Power-dividing coefficient

C_i Coupling coefficient

LIST OF ABBREVIATIONS

RF	Radio Frequency
TEM	Transverse Electro-magnetic
PCB	Printed Circuit Board
LHS	Left Hand Side
RHS	Right Hand Side
ADS	Advance Design System
EM	Electromagnetic
3D	Three-dimensional

CHAPTER 1

INTRODUCTION

Couplers are passive devices used in the field of radio technology. It couples a defined amount of the electromagnetic power in a transmission line to a port enabling the signal to be used in other circuits. The main application of a directional coupler is to pick off a small portion of the signal on a transmission line such that the incoming power can be actively monitored without too much loss.

There are two types of couplers waveguide type coupler and transmission line type coupler. In waveguide type couplers the waveguides are used for fabricating couplers. Some example of waveguide type couplers are

- Waveguide branch-line coupler,
- Bethe-hole directional coupler,
- Multihole waveguide Coupler
- Riblet short-slot coupler
- Schwinger reversed-phase coupler
- Moreno crossed-guide coupler

In transmission line type couplers the waveguides are used for fabricating couplers. Some example of transmission line type couplers are

- Branch-line coupler
- Lange coupler
- Hybrid coupler
- Hybrid ring coupler

In this study work is done on a coupled-line coupler. The Microstrip coupled-line couplers are the most important components in a RF system. When two transmission lines are placed close together with each other, because of the interaction of the electromagnetic fields of each transmission line, power can be coupled between

the transmission lines. These coupled lines are used to construct directional couplers. Generally, for designing of directional couplers microstrip and stripline forms are used. Although microstrip transmission lines do not support TEM and named as quasi-TEM, usually these are assumed to operate in TEM mode.

Microstrip coupled-line couplers [1] are widely used for the designs of different type of balanced power amplifiers, mixers, modulators, measurement systems, circularly polarized antennas, beam-forming array antennas, etc.

In practical applications, on the one hand, the coupling level of microstrip coupled- line coupler is mainly limited by the narrow separation between two parallel edge-coupled transmission lines, usually > 0.1 mm, in the PCB fabrication. On the other side, the poor directivity is mainly due to the difference in the phase velocities of even mode and odd mode on coupled microstrip lines.

1.1 Motivation

Couplers have been used extensively in a wide variety of microwave applications, including power division/combining and signal sampling. The majority of couplers provide coupling levels within the 8 – 40-dB range [1] while the measured directivity is usually smaller than 20 dB [2]. However, several applications require greater levels of coupling, up to 3-dB, which corresponds to division of incoming power into two equal halves and high directivity.

Therefore, the main limitations of the traditional coupled-line couplers are low coupling level and poor directivity in microstrip implementation. This motivated me to design such coupler which has great level of coupling and high directivity. In this work my aim is to design a coupler which has high directivity and tight coupling.

1.2 Research Objectives

The main limitations of the traditional coupled-line couplers are low coupling level and poor directivity in microstrip implementation. To achieve a tight coupling coefficient of 3 dB in microstrip coupled-line couplers, several methods have been

studied. Some techniques can achieve high directivity; however, the coupling coefficients are small or vice versa.

Although some methods can enhance the coupling performance, they may include some disadvantages such as inconvenient extra bonding wires, complicated design procedures or multilayer circuitries and large circuit areas. It is important that the directivity of these couplers is still poor.

Besides the coupling enhancement approaches, in order to improve the directivity of the microstrip coupled-line couplers, various kinds of compensation techniques have been investigated. These techniques include wigggle-line structure [15], velocities-compensation capacitors [16], [17] or inductors [2], additional output-ports matching networks [18], [19], and a combination of a regular microstrip and a negative-refractive-index line [20]. These techniques can achieve high directivity; however, the coupling coefficients are small.

The main objective of the research presented in this project to design a simple microstrip coupled line coupler without any extra bonding wires, complicated design procedures, patterned ground plane and which has high directivity and tight coupling.

1.3 Thesis Organization

Chapter 1 gives introduction about the couplers, motivation and objective of research of Coupled line coupler

Chapter 2 discussed the couplers also deals with the details about the research work carried out so far in designing of coupled line couplers.

Chapter 3 provides the details about the different basic parameters of coupler.

Chapter 4 describes about the coupled line coupler and design theory of the proposed coupler.

Chapter 5 discusses about the design, simulation and analysis result of microstrip coupled line coupler.

Chapter 6 concludes the thesis with comparison of result to some reported works and then suggestion for further research has discussed.

CHAPTER 2

LITERATURE REVIEW

2.1 Definition of Coupler

A coupler is a 4-port network that is designed to divide and distribute power. Couplers are passive devices used in the field of radio technology. Couplers couple a defined amount of the electromagnetic power in a transmission line to a port enabling the signal to be used in another circuit.

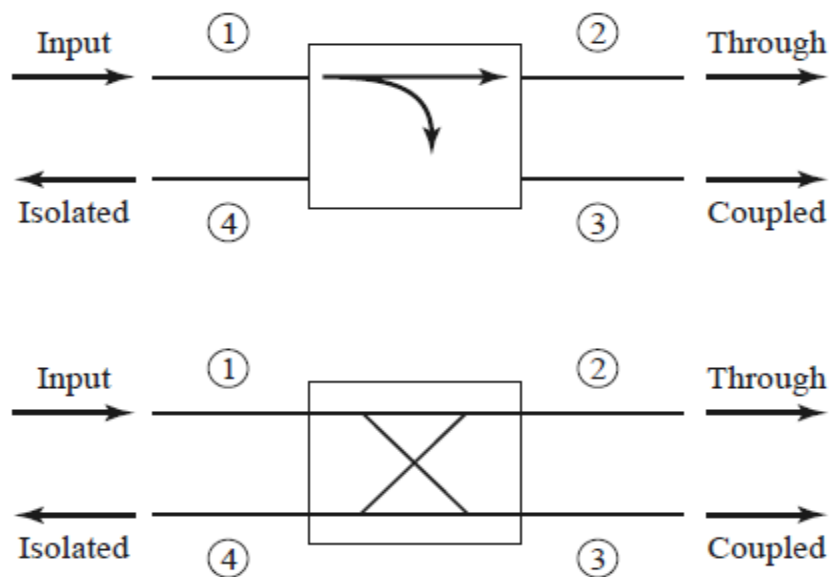


Figure 2.1: Commonly used symbols for directional couplers, and power flow conventions [21].

Couplers can be used in many applications, these include; providing a signal sample for measurement or monitoring, feedback, combining feeds to and from antennae, antenna beam forming, providing taps for cable distributed systems such as cable TV, and separating transmitted and received signals on telephone lines.

2.2 Literature Survey

The traditional coupled-line couplers have low coupling level and poor directivity in microstrip implementation. These are the main limitations of traditional coupled-line couplers. To achieve a tight coupling coefficient and high directivity in microstrip coupled-line couplers, several methods have been used. Some techniques can achieve high directivity; however, the coupling coefficients are small or vice versa.

To achieve a tight coupling coefficient of 3 dB in microstrip coupled-line couplers, several methods have been studied. Some techniques to increase coupling will be explained here.

Generally the coupling in a coupled line coupler is too loose to achieve coupling factors of 3 or 6 dB. One way to increase the coupling between edge-coupled lines is to use several lines parallel to each other, so that the fringing fields at both edges of a line contribute to the coupling. One of the most practical implementations of this idea is the *Lange type coupler* [3]. In this four parallel coupled lines are used with interconnections to provide tight coupling. The main disadvantage of the Lange coupler is probably practical, as the lines are very narrow and close together, and the required bonding wires across the lines increases complexity.

Other technique is by using microstrip tandem structure [4] we can increase the coupling of the coupler. But some time Tandem couplers require wiggles or serpentine, which make them very complex structure and these structures are not easy to realize.

Some other techniques are multilayer microstrip structure with broadside slot coupling with two elliptically shaped microstrip lines [5], Coupler using microstrip-to coplanar waveguide (CPW) via-hole transitions [6],[7] eliminates the requirement of bonding wires. But the holes make it a complex structure.

3-dB Quadrature Coupler Using Broadside-Coupled Coplanar Waveguides [8], Wideband tandem 3-dB coupler using a patterned ground plane [9] has 3 dB coupling but it uses patterned ground plane.

Vertically Installed Planar Couplers [10], Coupled-Line 3-dB Couplers Using Quarter-Wave Connecting Lines [11], Coupler using cascaded interconnecting coupled

lines and delay lines [12], Coupled-Line Coupler with High Coupling Level Using Shunt Periodic Stubs [13], Compact foldable coupled-line cascade couplers[14].

Although these methods can enhance the coupling performance, they may include some disadvantages such as inconvenient extra bonding wires [3], [4], complicated design procedures or multilayer circuitries [5–10], and large circuit areas [11–14]. It is important that the directivity of these couplers is still poor.

Besides the coupling enhancement approaches, in order to improve the directivity of the microstrip coupled-line couplers, various kinds of compensation techniques have been investigated.

These techniques include wobble-line structure [15], velocities- compensation capacitors [16], [17] or Inductor-Loaded Microstrip Directional Coupler for Directivity Enhancement [2], additional output-ports matching networks [18], [19], and a combination of a regular microstrip and a negative-refractive-index line [20],[21].

Wiggly line couplers use zig zag shape microstrip lines, which increases the complexity of the structure. These techniques can achieve high directivity; however, the coupling coefficients are small.

In this study, by combining two coupled-line sections, which are different from the non coupled connecting delay lines [11]–[14], a new coupled-line coupler with tight coupling coefficient and high-directivity performance is proposed, and this is suitable for microstrip PCB realization. Although all coupled lines in this proposed coupler are realized by loosely coupled microstrip structures, they can provide flexible parameters to enhance the coupling capability and compensate the difference between the phase velocities of the even and odd modes, simultaneously.

This proposed microstrip coupled-line coupler offers several advantages:

- 1) Tight coupling coefficients of almost 3 dB
- 2) Excellent full-wave simulated directivity
- 3) Without any via-holes or wire bonding
- 4) Easy realization in common microstrip technology with planar loosely coupled structure

- 5) Analytical design equations for initial circuit electrical parameters and scattering parameters
- 6) Symmetrical structure in a single layer with intact ground plane.

CHAPTER 3

BASIC PROPERTIES OF DIRECTIONAL COUPLER

A directional couplers or couplers are passive devices which couple part of the transmission power by a known amount out through another port, often by using two transmission lines placed close enough together such that energy passing through one transmission line is coupled to the other transmission.

Common properties desired for all the directional couplers are wide operational bandwidth, high directivity, and a good impedance match at all the ports when the other ports are terminated by matched loads.

3.1 Four-Port Networks

A coupler or directional coupler is a 4-port network. The scattering matrix of a reciprocal four-port network is

$$[S] = \begin{bmatrix} 0 & S_{12} & S_{13} & S_{14} \\ S_{12} & 0 & S_{23} & S_{24} \\ S_{13} & S_{23} & 0 & S_{34} \\ S_{14} & S_{24} & S_{34} & 0 \end{bmatrix} \quad (3.1)$$

If the network is matched at every port, then $S_{11} = S_{22} = S_{33} = S_{44} = 0$. If the network is reciprocal, then $S_{21} = S_{12}$, $S_{31} = S_{13}$, $S_{32} = S_{23}$, $S_{41} = S_{14}$, $S_{42} = S_{24}$, $S_{43} = S_{34}$.

If the network is lossless, 10 equations result from the unitarity, or energy conservation, condition [22]. Let us consider the multiplication of row 1 and row 2, and the multiplication of row 4 and row 3, also similarly, the multiplication of row 1 and row 3, and the multiplication of row 4 and row 2, give:

$$S_{13}^* S_{23} + S_{14}^* S_{23} = 0 \quad (3.2a)$$

$$S_{14}^* S_{13} + S_{24}^* S_{23} = 0 \quad (3.2b)$$

$$S_{12}^* S_{23} + S_{14}^* S_{34} = 0 \quad (3.2c)$$

$$S_{13}^* S_{23} + S_{14}^* S_{23} = 0 \quad (3.2d)$$

Now multiply (3.2a) by S_{24}^* , (3.2b) by S_{13}^* , (3.2c) by S_{12} and (3.2d) by S_{34} , and subtract to obtain:

$$S_{14}^* (|S_{13}|^2 - |S_{24}|^2) = 0 \quad (3.3)$$

$$S_{23} (|S_{12}|^2 - |S_{34}|^2) = 0 \quad (3.4)$$

We can satisfy (3.3) and (3.4) by one way if $S_{14} = S_{23} = 0$, which results in a direction coupler. Then the self-products of the rows of the unitary scattering matrix of (3.1) yield the following equations:

$$|S_{12}|^2 + |S_{13}|^2 = 1 \quad (3.5a)$$

$$|S_{12}|^2 + |S_{24}|^2 = 1 \quad (3.5b)$$

$$|S_{13}|^2 + |S_{34}|^2 = 1 \quad (3.5c)$$

$$|S_{24}|^2 + |S_{34}|^2 = 1 \quad (3.5d)$$

which imply that $|S_{13}| = |S_{24}|$ and $|S_{12}| = |S_{34}|$.

Further simplification can be made by choosing the phase references on three of the four ports. Thus, we choose $S_{12} = S_{34} = \alpha$, $S_{13} = \beta e^{j\theta}$, and $S_{24} = \beta e^{j\varphi}$, where α and β are real, and θ and φ are phase constants to be determined [21]. The dot product of rows 2 and 3 gives

$$S_{12}^* S_{13} + S_{24}^* S_{34} = 0 \quad (3.6)$$

which give a relation between phase constants

$$\theta + \varphi = \pi \pm 2n\pi \quad (3.7)$$

There are two commonly used realizations of directional couplers:

Symmetric Coupler:

$\theta = \varphi = \pi/2$. The phases of the terms having amplitude β are chosen equal. Then the S matrix has the following form:

$$[S] = \begin{bmatrix} 0 & \alpha & j\beta & 0 \\ \alpha & 0 & 0 & j\beta \\ j\beta & 0 & 0 & \alpha \\ 0 & j\beta & \alpha & 0 \end{bmatrix} \quad (3.8)$$

Asymmetric Coupler:

$\theta = 0, \varphi = \pi$. The phases of the terms having amplitude β are chosen to be 180. Then the S matrix has the following form:

$$[S] = \begin{bmatrix} 0 & \alpha & \beta & 0 \\ \alpha & 0 & 0 & -\beta \\ \beta & 0 & 0 & \alpha \\ 0 & -\beta & \alpha & 0 \end{bmatrix} \quad (3.9)$$

It is important to notice that the two couplers differ only in the choice of reference planes. Also, the amplitudes α and β are real numbers and are not independent:

$$\alpha^2 + \beta^2 = 1 \quad (3.10)$$

Thus the conclusion is that any reciprocal, lossless, matched four-port network is called directional coupler.

3.2 Directional couplers characterization

The basic operations of a directional coupler can be understood with the help of figure given below.

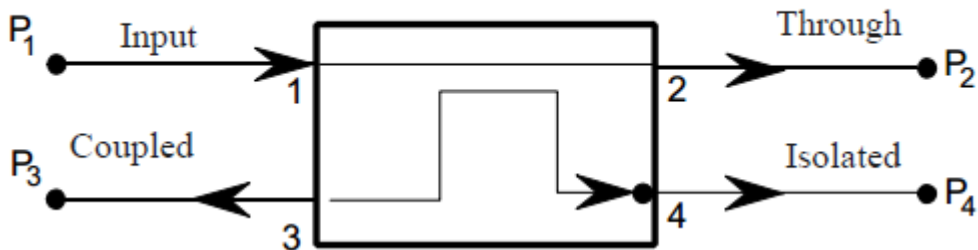


Figure 3.1 Basic block diagram of Direction Coupler

A directional coupler has four ports, defined as: Port 1 which is called *input port*, where we apply the signal, Port 2 which is called *through port*, where the output signal appears, Port 3 is called *coupled port*, where we obtain a sample of the input signal and Port 4 is called *isolated port*. In an ideal directional coupler, no power is delivered to isolated port (port 4).

The following quantities are commonly used to characterize a directional coupler:

3.2.1 Coupling C

The coupling factor indicates the fraction of the input power that is coupled to the coupled port (port 3). The coupling factor represents the primary property of a directional coupler. The expression for coupling is shown below.

$$\text{Coupling} = C \text{ (dB)} = 10 \log \frac{P_1}{P_3} = -20 \log S_{31} \text{ dB} \quad (3.11)$$

Where

P_1 = the input power at port 1

P_3 = the output power from the port 3 (coupled port)

Coupling is not constant, but varies with frequency. So that the directional coupler it is useful only in a range of frequencies, which we define as operating frequency.

3.2.2 Isolation I

Isolation of a directional coupler can be defined as the difference in signal levels in dB between the input port (port 1) and the isolated port (port 4) when the two other output ports are terminated by matched loads. The isolation is a measure of the power delivered to the uncoupled port. Isolation can also be defined between any two output ports.

$$\text{Isolation} = I \text{ (dB)} = 10 \log \frac{P_1}{P_4} = -20 \log S_{41} \text{ dB} \quad (3.12)$$

where

P_1 = the input power at port 1

P_4 = the output power from the port 4 (Isolated port)

The isolation between the input port (port 1) and the isolated ports may be different from the isolation between the two output ports. For example, the isolation between port 1 and port 4 can be 30 dB while the isolation between port 2 and port 3 can be a different value such as 25 dB. The isolation should be high as possible as. In practical the isolated port is never completely isolated. Some RF power will always be present on isolation port. Waveguide directional couplers have the best isolation.

3.2.3 Directivity D

The directivity is the ability to transfer power from the input port to the coupled port. Directivity is a measure of how well the coupler isolates two opposite-travelling (forward and reverse) signals.

$$\text{Directivity} = D \text{ (dB)} = 10 \log \frac{P_3}{P_4} = 20 \log \frac{S_{31}}{S_{41}} \text{ dB} \quad (3.13)$$

Where

P_3 = the output power from the port 3 (coupled port)

P_4 = the output power from the port 4 (Isolated port)

The directivity should be high as possible as. The ideal coupler has infinite directivity. Waveguide directional couplers will have the best directivity. Directivity cannot be measured directly, and is calculated from the isolation and coupling measurements as:

$$D \text{ (dB)} = I \text{ (dB)} - C \text{ (dB)} \quad (3.14)$$

3.2.4 Insertion Loss

The insertion loss accounts for the input power delivered to the through port, diminished by power delivered to the coupled and isolated ports. In an ideal directional coupler, the main line loss port 1 to port 2 due to power coupled to the coupled output port is:

$$\text{Insertion Loss} = \text{IL (dB)} = 10 \log \frac{P_1}{P_2} = -20 \log S_{21} \text{ dB} \quad (3.13)$$

where

P_1 = the input power at port 1

P_2 = the power at port 2

The actual directional coupler losses will be a combination of coupling loss, dielectric loss, conductor loss, and VSWR loss. Depending on the frequency range, coupling losses become less significant above 15 dB coupling where the other losses constitute the majority of the total loss.

Table 3.1: Coupling Insertion Loss

Coupling (dB)	Insertion Loss (db)
3	3.00
6	1.25
10	0.458
20	0.0436
30	0.00435

CHAPTER 4

COUPLED-LINE COUPLER AND ITS DESIGN THEORY

4.1 Microstrip Line

Microstrip line is very popular types of planar transmission lines. A microstrip transmission line consists of a track of copper or other metal on a dielectric material. There is a "backplane" on the other side of the dielectric substrate, formed from a similar conductor. It can be manufactured by photolithographic processes and it is easy to miniaturize and integrate microstrip line with both passive and active microwave devices.

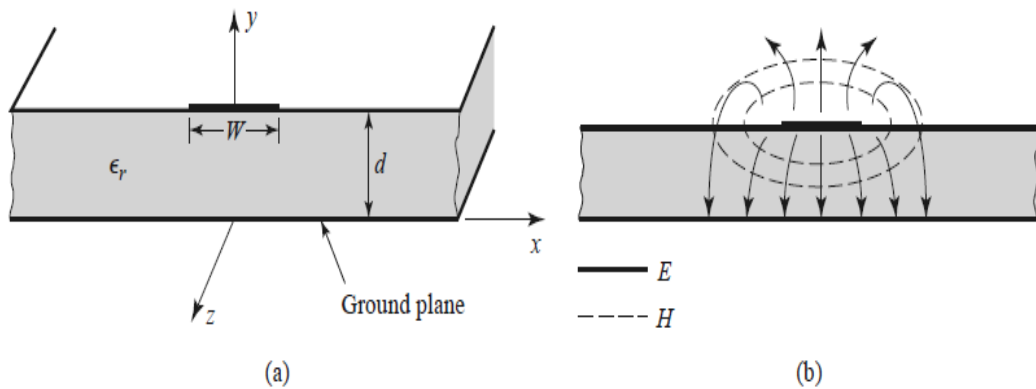


Figure 4.1: Microstrip transmission line. (a) Geometry. (b) Electric and magnetic field lines [21]

If there is no dielectric substrate ($\epsilon_r = 1$), we would have a two-wire transmission line consisting of a flat strip conductor over a ground plane, embedded in a homogeneous dielectric medium (air). This would constitute a very simple TEM transmission line.

In microstrip line above the strip there is air and below the strip there is dielectric material, so there is no homogeneous medium. This complicates the behaviour and analysis of microstrip line. Microstrip has some of its field lines in the dielectric medium between the strip conductor and the ground plane and some part in the air region above the substrate. Due to this microstrip line cannot support a pure TEM wave since the phase velocity of TEM field lines in the dielectric region would be $c/\sqrt{\epsilon_r}$, while the phase velocity of TEM field lines in the air would be c , so a phase-matching condition at the dielectric–air interface would be impossible to enforce [21].

4.2 Coupled Line

When two unshielded transmission lines are placed very close to each other, power can be coupled from one transmission line to the other due to the interaction of the electromagnetic fields. Such lines are called *coupled transmission lines*, and they normally consist of three conductors placed very close to each other, although more conductors can be used.

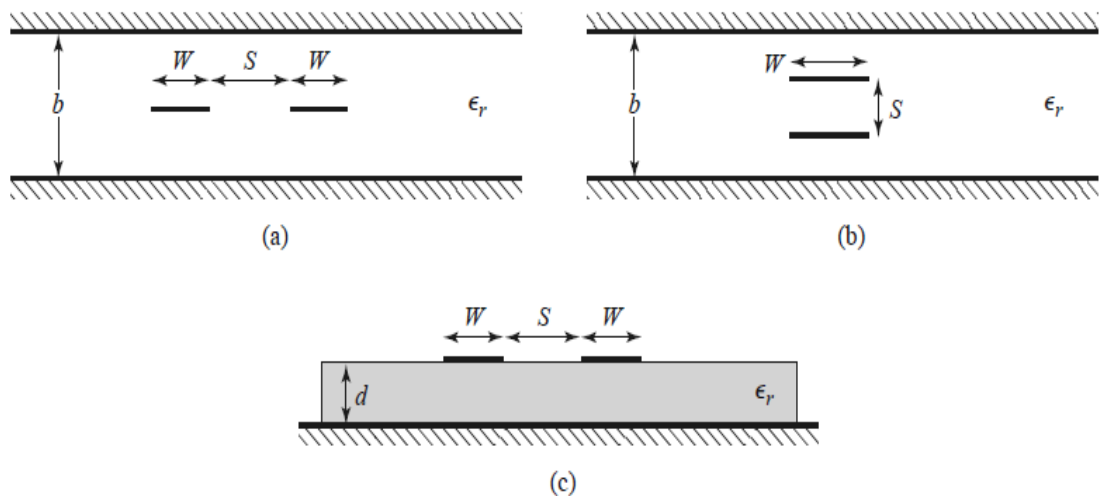


Figure 4.2: Various coupled transmission line geometries. (a) Coupled stripline (planar, or edge-coupled). (b) Coupled stripline (stacked, or broadside-coupled). (c) Coupled microstrip lines. [21]

4.2.1 Coupled Line Theory

The coupled lines of Figure 4.2 can be represented by the structure and equivalent circuit shown in Figure 4.3.

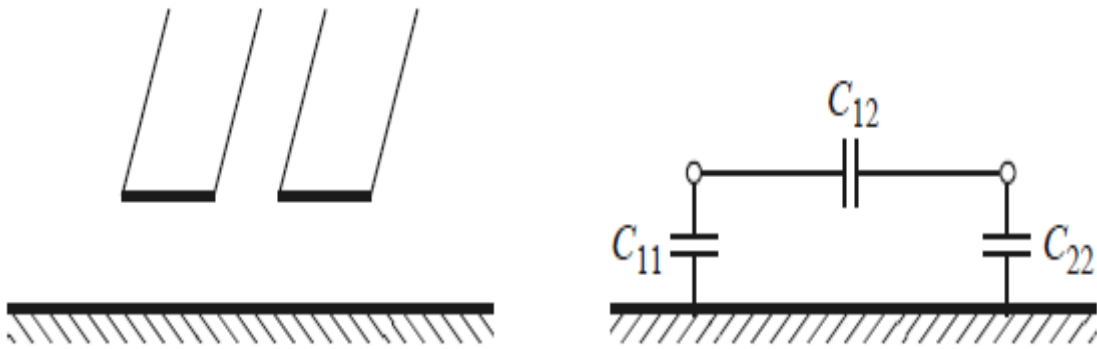


Figure 4.3: A three-wire coupled transmission line and its equivalent capacitance network. [21]

If we suppose TEM propagation, then the electrical characteristics of the coupled lines can be completely obtained from the effective capacitances between the transmission lines and the velocity of propagation on the transmission line. As shown in Figure 4.3, C_{12} represents the capacitance between two strip conductors, and C_{11} and C_{22} represent the capacitance between one strip conductor and ground. Because the strip lines are same in size and location relative to the ground conductor, we have $C_{11} = C_{22}$.

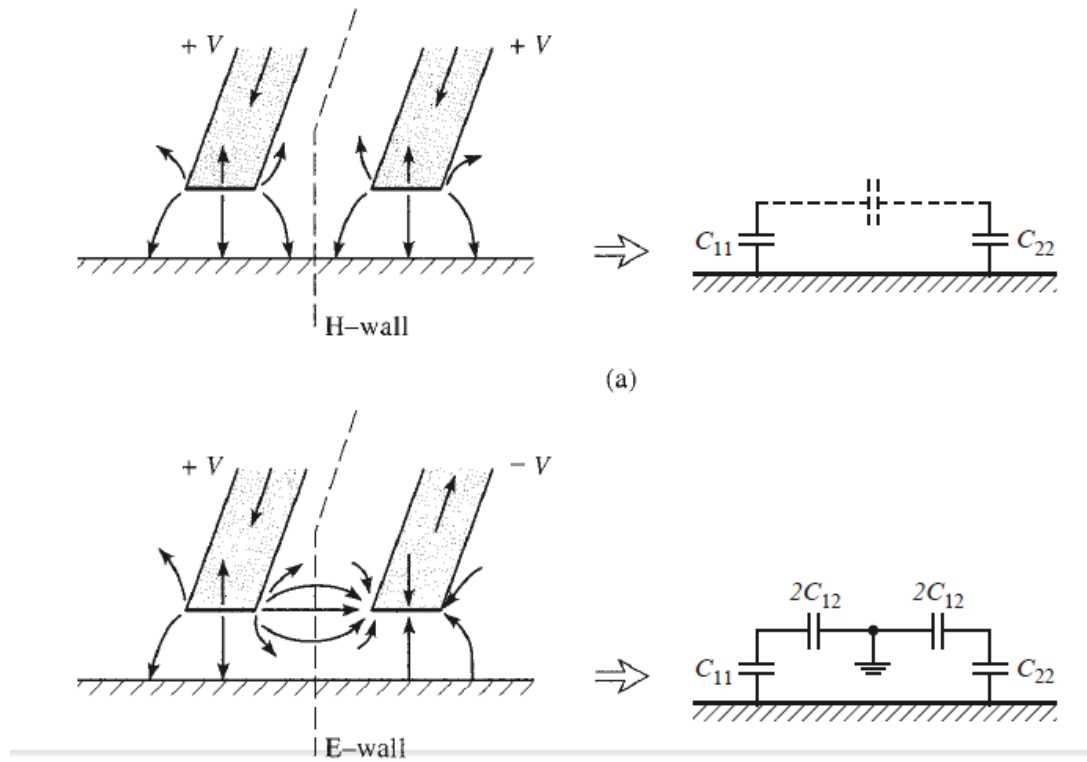


Figure 4.4: Even- and odd-mode excitations for a coupled line, and the resulting equivalent capacitance networks. (a) Even-mode excitation. (b) Odd-mode excitation. [21]

Now we take into consideration two special types of excitations for these coupled line: the *even mode*, here the currents in the strip conductors are in the same direction and equal in amplitude and the *odd mode*, here the currents in the strip conductors are equal in amplitude but in opposite directions. [21]

For *Even mode*, the electric field lines have even symmetry about the center line, and so there is no current flow between the two strip conductors. This leads to the equivalent circuit shown in figure 4.2(a), where C_{12} is effectively open-circuited. The resulting capacitance of either line to ground for the even mode is

$$C_e = C_{11} = C_{22} \quad (4.1)$$

If these two strip lines are identical in size and location. Then the characteristic impedance for even mode is

$$Z_{0e} = \sqrt{\frac{L_e}{C_e}} = \frac{\sqrt{L_e C_e}}{C_e} = \frac{1}{v_p C_e} \quad (4.2)$$

where $v_p = \frac{c}{\sqrt{\epsilon_r}} = \frac{1}{\sqrt{L_e C_e}} = \frac{1}{\sqrt{L_o C_o}}$ is the phase velocity of propagation on the transmission line.

For *Odd mode*, the electric field has an odd symmetry about the center line, and a voltage null exists between the two strip lines. We can imagine it as a ground plane through the middle of C_{12} , which leads to the equivalent circuit shown 4.2(b). In this case the effective capacitance between either strip line or ground is

$$C_o = C_{11} + 2C_{12} = C_{22} + 2C_{12} \quad (4.3)$$

and the characteristic impedance for the odd mode is

$$Z_{0o} = \sqrt{\frac{L_o}{C_o}} = \frac{\sqrt{L_o C_o}}{C_o} = \frac{1}{v_p C_o} \quad (4.4)$$

In words, Z_{0e} (Z_{0o}) is the characteristic impedance of one of the strip lines relative to ground when the coupled line is operated in the even (odd) mode. An arbitrary excitation of a coupled line can always be treated as a superposition of appropriate amplitudes of even- and odd-mode excitations [21].

4.3 Design Calculation for Proposed Coupler

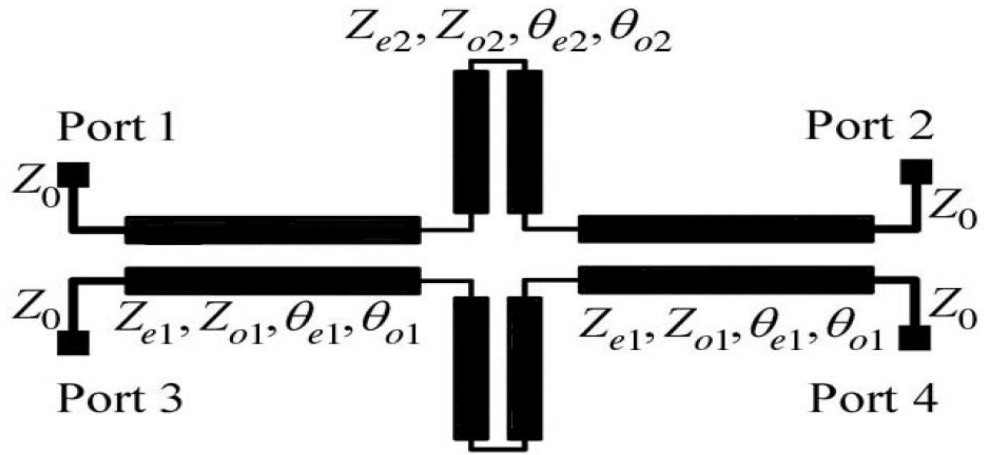


Figure 4.5: Circuit Schematic of the proposed Coupler

The scattering parameters of the proposed coupled-line coupler can be expressed in terms of its corresponding single-port circuits.

Case 1.

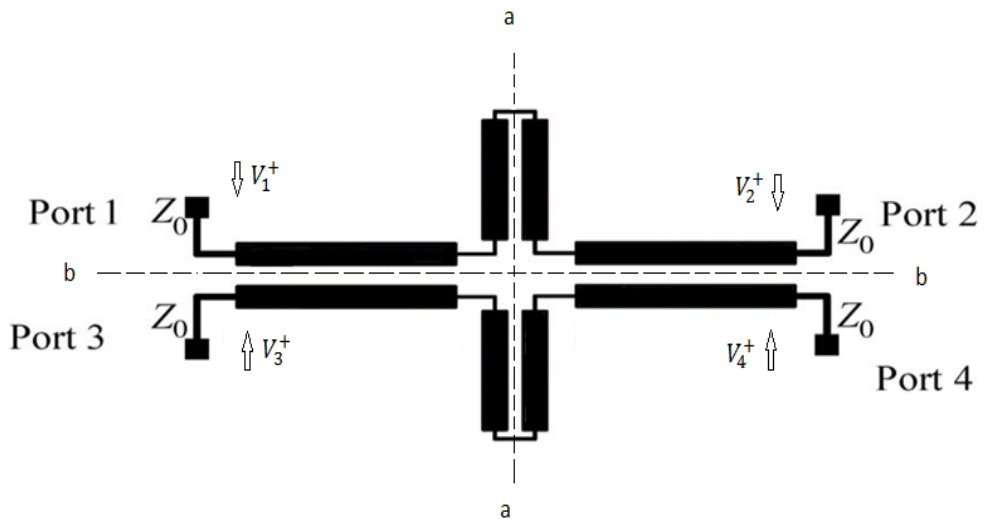


Figure 4.6: Even-even mode excitation

$$V_1^+ = V_2^+ = V_3^+ = V_4^+ = V^+ \quad (4.5)$$

For this case both symmetry planes correspond to magnetic walls, so this is even-even mode.

Case 2.

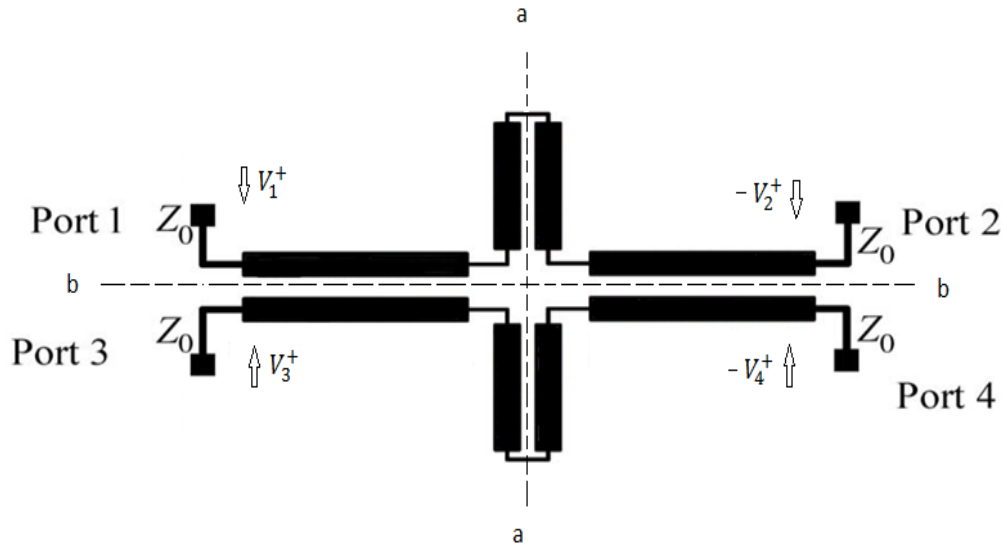


Figure 4.7: Even-Odd Mode excitation

$$V_1^+ = V_3^+ = V^+ \quad (4.6a)$$

$$V_2^+ = V_4^+ = -V^+ \quad (4.6b)$$

For this case plane bb is a magnetic wall and plane aa is an electric wall, so this is even odd mode.

Case 3.

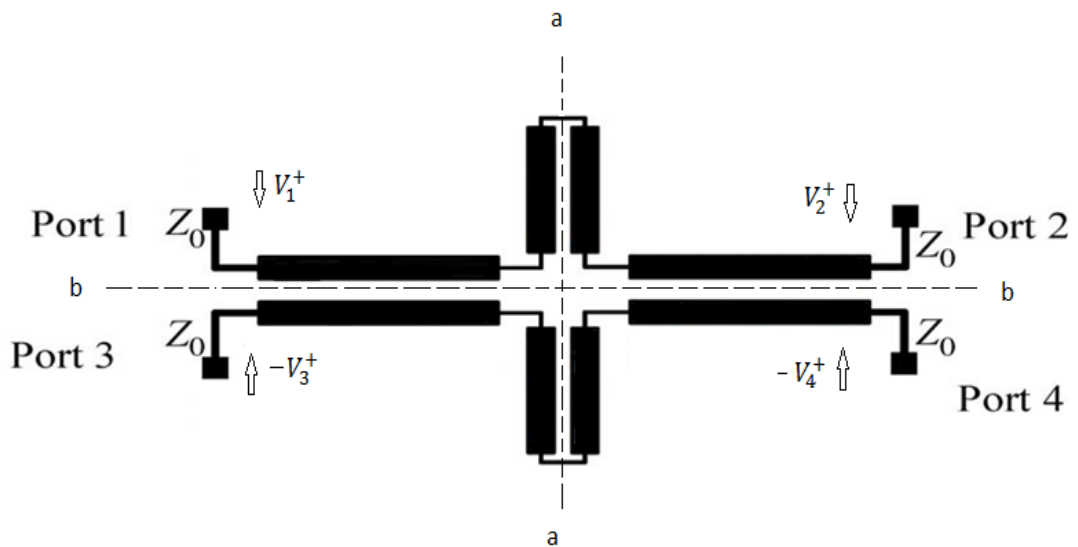


Figure 4.8: Odd-Even Mode excitation

$$V_1^+ = -V_3^+ = V^+ \quad (4.7a)$$

$$V_2^+ = -V_4^+ = V^+ \quad (4.7b)$$

For this case plane bb is an electric wall and plane aa is a magnetic wall, so this is odd even mode.

Case 4.

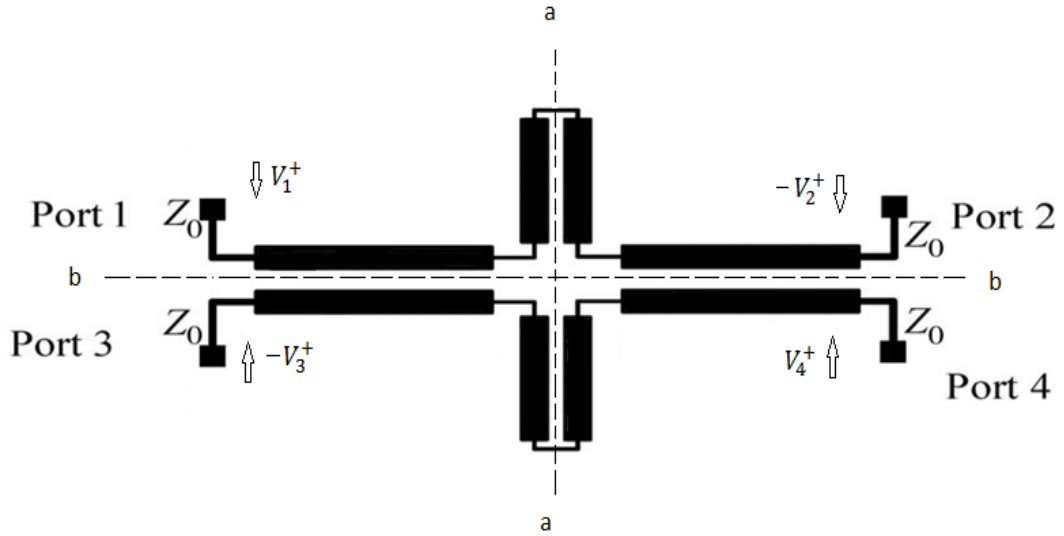


Figure 4.9: Odd-Odd Mode excitation

$$V_1^+ = -V_3^+ = V^+ \quad (4.8a)$$

$$V_2^+ = -V_4^+ = -V^+ \quad (4.8b)$$

For this case both symmetry planes correspond to electric walls, so this is odd - odd mode.

For case 1 from symmetry consideration we have reflected voltage from each port.

$$V_1^- = \Gamma_{ee} V^+ \quad (4.9a)$$

$$V_2^- = \Gamma_{ee} V^+ \quad (4.9b)$$

$$V_3^- = \Gamma_{ee} V^+ \quad (4.9c)$$

$$V_4^- = \Gamma_{ee} V^+ \quad (4.9d)$$

For case 2 from symmetry consideration we have reflected voltage from each port.

$$V_1^- = \Gamma_{eo} V^+ \quad (4.10a)$$

$$V_2^- = -\Gamma_{eo} V^+ \quad (4.10b)$$

$$V_3^- = \Gamma_{eo} V^+ \quad (4.10c)$$

$$V_4^- = -\Gamma_{eo} V^+ \quad (4.10d)$$

For case 3 from symmetry consideration we have reflected voltage from each port.

$$V_1^- = \Gamma_{oe} V^+ \quad (4.11a)$$

$$V_2^- = \Gamma_{oe} V^+ \quad (4.11b)$$

$$V_3^- = -\Gamma_{oe} V^+ \quad (4.11c)$$

$$V_4^- = -\Gamma_{oe} V^+ \quad (4.11d)$$

For case 4 from symmetry consideration we have

$$V_1^- = \Gamma_{oo} V^+ \quad (4.12a)$$

$$V_2^- = -\Gamma_{oo} V^+ \quad (4.12b)$$

$$V_3^- = -\Gamma_{oo} V^+ \quad (4.12c)$$

$$V_4^- = \Gamma_{oo} V^+ \quad (4.12d)$$

We now superimpose these four solutions. The superposition of the four incident waves at each port gives $V_1^+ = V^+$, $V_2^+ = V_3^+ = V_4^+ = 0$. thus only port 1 is excited. The superposition of the reflected waves gives

$$V_1^- = (\Gamma_{ee} + \Gamma_{eo} + \Gamma_{oe} + \Gamma_{oo}) V^+$$

$$V_1^- = \frac{1}{4}(\Gamma_{ee} + \Gamma_{eo} + \Gamma_{oe} + \Gamma_{oo}) V_1^+ \quad (4.13)$$

So

$$S_{11} = \frac{V_1^-}{V_1^+} = \frac{1}{4}(\Gamma_{ee} + \Gamma_{eo} + \Gamma_{oe} + \Gamma_{oo}) \quad (4.14a)$$

Similarly

$$S_{21} = \frac{V_2^-}{V_1^+} = \frac{1}{4}(\Gamma_{ee} - \Gamma_{eo} + \Gamma_{oe} - \Gamma_{oo}) \quad (4.14b)$$

$$S_{31} = \frac{V_3^-}{V_1^+} = \frac{1}{4}(\Gamma_{ee} + \Gamma_{eo} - \Gamma_{oe} - \Gamma_{oo}) \quad (4.14c)$$

$$S_{41} = \frac{V_4^-}{V_1^+} = \frac{1}{4}(\Gamma_{ee} - \Gamma_{eo} - \Gamma_{oe} + \Gamma_{oo}) \quad (4.14d)$$

Thus due to the symmetry feature in the planar structure, (4.14) can completely represent other scattering parameters values of the proposed couple-line coupler

$$S_{11} = \frac{\Gamma_{ee} + \Gamma_{eo} + \Gamma_{oe} + \Gamma_{oo}}{4} \quad (4.15a)$$

$$S_{21} = \frac{\Gamma_{ee} - \Gamma_{eo} + \Gamma_{oe} - \Gamma_{oo}}{4} \quad (4.15b)$$

$$S_{31} = \frac{\Gamma_{ee} + \Gamma_{eo} - \Gamma_{oe} - \Gamma_{oo}}{4} \quad (4.15c)$$

$$S_{41} = \frac{\Gamma_{ee} - \Gamma_{eo} - \Gamma_{oe} + \Gamma_{oo}}{4} \quad (4.15d)$$

Here $\Gamma_{ee}, \Gamma_{eo}, \Gamma_{oe}, \Gamma_{oo}$ are the input reflection coefficients for the even–even, even–odd, odd–even, and odd–odd mode equivalent circuits.

For mathematical simplification, all characteristic impedance values are normalized with respect to the port impedance Z_o , which is expressed as

$$z_{e1} = \frac{Z_{e1}}{Z_o}; \quad z_{o1} = \frac{Z_{o1}}{Z_o}; \quad z_{e2} = \frac{Z_{e2}}{Z_o}; \quad z_{o2} = \frac{Z_{o2}}{Z_o} \quad (4.16)$$

Based on the conventional transmission-line theory, the input reflection coefficients can be calculated as

$$\Gamma_{ee} = \frac{Z_{inee} - 1}{Z_{inee} + 1} \quad (4.17a)$$

$$\Gamma_{eo} = \frac{Z_{ineo} - 1}{Z_{ineo} + 1} \quad (4.17b)$$

$$\Gamma_{oe} = \frac{Z_{inoe} - 1}{Z_{inoe} + 1} \quad (4.17c)$$

$$\Gamma_{oo} = \frac{Z_{inoo} - 1}{Z_{inoo} + 1} \quad (4.17d)$$

Where z_{inee} , z_{ineo} , z_{inoe} , z_{inoo} are input impedances for even-even, even-odd, odd-even, odd-odd mode respectively.

These input impedances can be calculated using conventional transmission-line input impedance formula.

$$z_{in} = z_0 \left[\frac{z_L + jz_0 \tan \theta}{z_0 + jz_L \tan \theta} \right] \quad (4.18)$$

I. For even-even mode



Figure 4.10: Even-Even Mode

For this case

$$z_L = -jz_{e2} \cot(\theta_{e2})$$

$$z_0 = z_{e1}$$

$$\theta = \theta_{e1}$$

On putting these values in equation (4.18) we get

$$\begin{aligned} z_{inee} &= z_{e1} \left[\frac{-jz_{e2} \cot(\theta_{e2}) + jz_{e1} \tan(\theta_{e1})}{z_{e1} + z_{e2} \cot(\theta_{e2}) \tan(\theta_{e1})} \right] \\ z_{inee} &= j z_{e1} \left[\frac{-z_{e2} + z_{e1} \tan(\theta_{e1}) \tan(\theta_{e2})}{z_{e1} \tan(\theta_{e2}) + z_{e2} \tan(\theta_{e1})} \right] \\ z_{inee} &= j z_{e1} \frac{z_{e1} \tan(\theta_{e1}) \tan(\theta_{e2}) - z_{e2}}{z_{e1} \tan(\theta_{e2}) + z_{e2} \tan(\theta_{e1})} \end{aligned} \quad (4.19)$$

II. For Even-Odd Mode

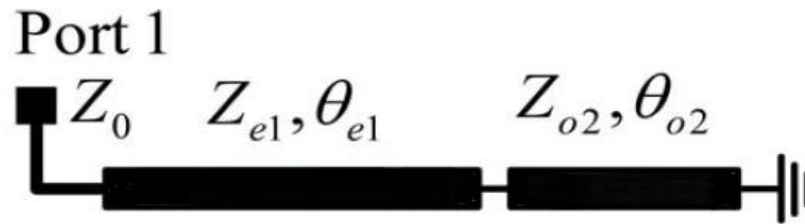


Figure 4.11: Even-Odd Mode

For this case

$$z_L = jz_{o2} \tan(\theta_{o2})$$

$$z_0 = z_{e1}$$

$$\theta = \theta_{e1}$$

On putting these values in equation (4.18) we get

$$z_{ineo} = z_{e1} \left[\frac{jz_{o2} \tan(\theta_{o2}) + z_{e1} \tan(\theta_{e1})}{z_{e1} - z_{o2} \tan(\theta_{e1}) \tan(\theta_{o2})} \right]$$

$$z_{ineo} = j z_{e1} \left[\frac{z_{e2} \tan(\theta_{o2}) + z_{e1} \tan(\theta_{e1})}{z_{e1} - z_{o2} \tan(\theta_{e1}) \tan(\theta_{o2})} \right]$$

$$z_{ineo} = j z_{e1} \frac{z_{e1} \tan(\theta_{e1}) + z_{o2} \tan(\theta_{o2})}{z_{e1} - z_{o1} \tan(\theta_{e1}) \tan(\theta_{o2})} \quad (4.20)$$

III. For Odd-Even Mode

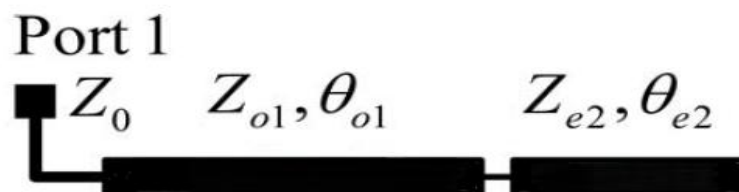


Figure 4.12: Odd-Even Mode

$$z_L = -jz_{e2} \cot(\theta_{e2})$$

$$z_0 = z_{o1}$$

$$\theta = \theta_{o1}$$

On putting these values in equation (4.18) we get

$$z_{inoe} = z_{o1} \left[\frac{-jz_{e2} \cot(\theta_{e2}) + jz_{o1} \tan(\theta_{o1})}{z_{o1} + z_{e2} \cot(\theta_{e2}) \tan(\theta_{o1})} \right]$$

$$z_{inoe} = j z_{e1} \left[\frac{-z_{e2} + z_{o1} \tan(\theta_{o1}) \tan(\theta_{e2})}{z_{o1} \tan(\theta_{e2}) + z_{e2} \tan(\theta_{o1})} \right]$$

$$z_{inoe} = j z_{o1} \frac{z_{o1} \tan(\theta_{o1}) \tan(\theta_{e2}) - z_{e2}}{z_{o1} \tan(\theta_{e2}) + z_{e2} \tan(\theta_{o1})} \quad (4.21)$$

VI. For Odd-Odd Mode

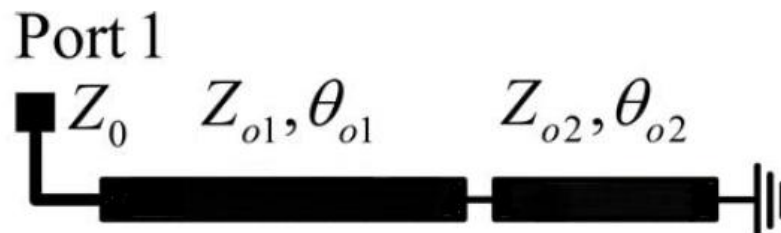


Figure 4.13: Odd-Odd Mode

For this case

$$z_L = jz_{o2} \tan(\theta_{e2})$$

$$z_0 = z_{o1}$$

$$\theta = \theta_{o1}$$

On putting these values in equation (4.18) we get

$$z_{inoo} = z_{o1} \left[\frac{jz_{o2} \tan(\theta_{o2}) + jz_{o1} \tan(\theta_{o1})}{z_{o1} - z_{o2} \tan(\theta_{o1}) \tan(\theta_{o2})} \right]$$

$$Z_{inoo} = j Z_{o1} \left[\frac{z_{o2} \tan(\theta_{o2}) + z_{o1} \tan(\theta_{o1})}{z_{o1} - z_{o2} \tan(\theta_{o1}) \tan(\theta_{o2})} \right]$$

$$Z_{inoo} = j Z_{o1} \frac{z_{o1} \tan(\theta_{o1}) + z_{o2} \tan(\theta_{o2})}{z_{o1} - z_{o2} \tan(\theta_{o1}) \tan(\theta_{o2})} \quad (4.22)$$

For perfect input-port matching S_{11} should be zero, so

$$\Gamma_{ee} + \Gamma_{eo} + \Gamma_{oe} + \Gamma_{oo} = 0 \quad (4.23)$$

For perfect isolation S_{41} should be zero, so

$$\Gamma_{ee} - \Gamma_{eo} - \Gamma_{oe} + \Gamma_{oo} = 0 \quad (4.24)$$

On adding equation (4.23) and (4.24) we get

$$\Gamma_{ee} + \Gamma_{oo} = 0 \quad (4.25a)$$

On subtracting equation (4.24) from (4.23) equation we get

$$\Gamma_{eo} + \Gamma_{oe} = 0 \quad (4.25b)$$

After combining (4.17) and (4.25), we can obtain

$$Z_{inee} Z_{inoo} = Z_{ineo} Z_{inoe} = 1 \quad (4.26)$$

If a 90° coupler with arbitrary power division is designed, the relationship of the coupling and transmission parameters should be

$$S_{21} = jkS_{31} \quad (4.27)$$

where k is the power-dividing coefficient. Similarly, after combining (4.15), (4.17), and (4.27), another important equation can be found as

$$kj (Z_{inee} Z_{ineo} - 1) = Z_{inee} - Z_{inoo} \quad (4.28)$$

To solve these nonlinear equations the following constrains are assumed for the initial design:

$$\theta_1 = \theta_{e1} = \theta_{o1} ; \theta_2 = \theta_{e2} = \theta_{o2} \quad (4.29a)$$

$$0 < \theta_1 \leq 90^0 ; 0 < \theta_2 \leq 90^0 \quad (4.29b)$$

After considering (4.29), there are two different cases to solve (4.26) and (4.28).

Case I When $\theta = 90^0$

By substituting (4.29a) and $\theta = 90^\circ$ into (4.19), (4.20), (4.21), (4.22) the following four relationships can be obtained:

$$Z_{inee} = \frac{jZ_{e1}^2 \tan(\theta_2)}{z_{e2}} \quad (4.30a)$$

$$Z_{ineo} = \frac{-jZ_{e1}^2}{z_{o2} \tan(\theta_2)} \quad (4.30b)$$

$$Z_{inoe} = \frac{jZ_{o1}^2 \tan(\theta_2)}{z_{e2}} \quad (4.30c)$$

$$Z_{inoo} = \frac{-jZ_{o1}^2}{z_{o2} \tan(\theta_2)} \quad (4.30d)$$

On combining equation (4.26) and (4.30) we get

$$\left(\frac{-jZ_{e1}^2}{z_{o2} \tan(\theta_2)}\right) \cdot \left(\frac{jZ_{o1}^2 \tan(\theta_2)}{z_{e2}}\right) = 1$$

$$\frac{z_{e1}^2 z_{o1}^2}{z_{o2} z_{e2}} = 1$$

$$z_{e1}^2 z_{o1}^2 = z_{e2} z_{o2} \quad (4.31a)$$

Using equation (4.28) and (4.30) we get

$$kj \left(\frac{jZ_{e1}^2 \tan(\theta_2)}{z_{e2}} \cdot \frac{-jZ_{e1}^2}{z_{o2} \tan(\theta_2)} - 1\right) = \frac{jz_{e1}^2 \tan(\theta_2)}{z_{e2}} - \frac{-jz_{e1}^2}{z_{o2} \tan(\theta_2)}$$

$$k(z_{e1}^4 - z_{e2} z_{o2}) \tan(\theta_2) = z_{e1}^2 z_{o2} \tan^2(\theta_2) + z_{e1}^2 z_{e2} \quad (4.31b)$$

There are five unknowns, i.e., z_{o1} , z_{e1} , z_{e2} , z_{o2} and θ_2 , but we have two conditions of (4.31). For this θ_2 , z_{e1} and z_{o1} are assumed as known parameters. Now we can solve two conditions of (4.31) and get z_{o2} and z_{e2} .

From equation (4.31) we get

$$z_{o2} = \frac{z_{e1}^2 z_{o1}^2}{z_{e2}} \quad (4.32a)$$

$$z_{e2} = \frac{k(z_{e1}^4 - z_{e2} z_{o2}) \tan(\theta_2) - z_{e1}^2 z_{o2} \tan^2(\theta_2)}{z_{e1}^2} \quad (4.32b)$$

On putting the value of z_{o2} in equation (4.32b)

$$z_{e2} = \frac{k(z^4_{e1} - z^2_{e1}z^2_{o1}) - \frac{z^4_{e1}z^2_{o1}}{z_{e2}} \tan(\theta_2)}{z^2_{e1} \cot(\theta_2)}$$

$$z_{e2} = \frac{k(z^4_{e1} - z^2_{e1}z^2_{o1})z_{e2} - z^4_{e1}z^2_{o1} \tan(\theta_2)}{z^2_{e1}z_{e2} \cot(\theta_2)}$$

$$z^2_{e1}z^2_{e2} \cot(\theta_2) - kz^2_{e1}(z^2_{e1} - z^2_{o1})z_{e2} + z^4_{e1}z^2_{o1} \tan(\theta_2) = 0 \quad (4.33)$$

This is a quadratic equation and the solution of quadratic equation is $x = \frac{-b \pm \sqrt{b^2 - 4ac}}{2a}$

So,

$$a = z^2_{e1} \cot(\theta_2)$$

$$b = -kz^2_{e1}(z^2_{e1} - z^2_{o1})$$

$$c = z^4_{e1}z^2_{o1} \tan(\theta_2)$$

On putting these values into the solution of quadratic equation, we get

$$z_{e2} = \frac{kz^2_{e1}(z^2_{e1} - z^2_{o1}) \pm \sqrt{k^2z^4_{e1}(z^2_{e1} - z^2_{o1})^2 - 4z^6_{e1}z^2_{o1}}}{2z^2_{e1} \cot(\theta_2)} \quad (4.34a)$$

Similarly we can find z_{o2}

$$z_{o2} = \frac{kz^2_{e1}(z^2_{e1} - z^2_{o1}) \pm \sqrt{k^2z^4_{e1}(z^2_{e1} - z^2_{o1})^2 - 4z^6_{e1}z^2_{o1}}}{2z^2_{e1} \tan(\theta_2)} \quad (4.34b)$$

Here we have four solution, but only two solution satisfy the conditions of equation (4.31) and these solutions are

$$z_{e2} = \frac{kz^2_{e1}(z^2_{e1} - z^2_{o1}) + \sqrt{k^2z^4_{e1}(z^2_{e1} - z^2_{o1})^2 - 4z^6_{e1}z^2_{o1}}}{2z^2_{e1} \cot(\theta_2)} \quad (4.35a)$$

$$z_{o2} = \frac{kz^2_{e1}(z^2_{e1} - z^2_{o1}) - \sqrt{k^2z^4_{e1}(z^2_{e1} - z^2_{o1})^2 - 4z^6_{e1}z^2_{o1}}}{2z^2_{e1} \tan(\theta_2)} \quad (4.35b)$$

Now we assume that θ_2 , z_{e2} and z_{o2} are the known parameters and we can solve two conditions of (4.31) for z_{o1} and z_{e1} .

From equation (4.31) we get

$$z^2_{e1} = \frac{z_{e2} z_{o2}}{z^2_{e1}}$$

On putting the value of z^2_{e1} in (4.31b) we get

$$k \left[\frac{z_{e2}^2 z_{o2}^2}{z_{o1}^4} - z_{e2} z_{o2} \right] \tan(\theta_2) = \frac{z_{e2} z_{o2}}{z_{o1}^2} \cdot z_{o2} \tan^2(\theta_2) + \frac{z_{e2} z_{o2}}{z_{o1}^2} \cdot z_{e2}$$

$$k z_{e2} z_{o2} z_{o1}^4 \tan(\theta_2) + [z_{o2} \tan^2(\theta_2) + z_{e2}] z_{e2} z_{o2} z_{o1}^2 - k z_{e2}^2 z_{o2}^2 \tan(\theta_2) = 0 \quad (4.36)$$

This is a quadratic equation in term of z_{o1}^2 and the solution of quadratic equation is $x = \frac{-b \pm \sqrt{b^2 - 4ac}}{2a}$

Here

$$a = k z_{e2} z_{o2} \tan(\theta_2)$$

$$b = [z_{o2} \tan^2(\theta_2) + z_{e2}] z_{e2} z_{o2}$$

$$c = -k z_{e2}^2 z_{o2}^2 \tan(\theta_2)$$

On putting these values into the solution of quadratic equation, we get

$$z_{o1}^2 = \frac{-[z_{o2} \tan^2(\theta_2) + z_{e2}] z_{e2} z_{o2} \pm \sqrt{[(\tan^2(\theta_2) + z_{e2}) z_{e2} z_{o2}]^2 + 4k^2 z_{e2}^3 z_{o2}^3 \tan^2(\theta_2)}}{2k z_{e2} z_{o2} \tan(\theta_2)}$$

$$z_{o1}^2 = \frac{-[z_{o2} \tan^2(\theta_2) + z_{e2}] z_{e2} z_{o2} \pm \sqrt{[(\tan^2(\theta_2) + z_{e2})]^2 + 4k^2 z_{e2} z_{o2} \tan^2(\theta_2)}}{2k \tan(\theta_2)} \quad (4.37a)$$

Similarly we can find z_{e1}^2

$$z_{e1}^2 = \frac{[z_{o2} \tan^2(\theta_2) + z_{e2}] \pm \sqrt{[(\tan^2(\theta_2) + z_{e2})]^2 + 4k^2 z_{e2} z_{o2} \tan^2(\theta_2)}}{2k \tan(\theta_2)} \quad (4.37b)$$

Here we have four solution, but only two solution satisfy the conditions of equation (4.31) and these solutions are

$$z_{e1} = \sqrt{\frac{\sqrt{[(\tan^2(\theta_2) + z_{e2})]^2 + 4k^2 z_{e2} z_{o2} \tan^2(\theta_2)} + [z_{o2} \tan^2(\theta_2) + z_{e2}]}{2k \tan(\theta_2)}} \quad (4.38a)$$

$$z_{o1} = \sqrt{\frac{\sqrt{[(\tan^2(\theta_2) + z_{e2})]^2 + 4k^2 z_{e2} z_{o2} \tan^2(\theta_2)} + [z_{o2} \tan^2(\theta_2) + z_{e2}]}{2k \tan(\theta_2)}} \quad (4.38b)$$

Case I When $\theta \neq 90^\circ$

In this case, the electrical lengths of two-section coupled lines are not fixed and the solutions are more general.

From equation (4.26)

$$z_{inee} z_{inoo} = 1$$

Now put the value of z_{inee} and z_{inoo} from (4.19) and (4.22) in above equation

$$\left[j z_{e1} \frac{z_{e1} \tan(\theta_1) \tan(\theta_2) - z_{e2}}{z_{e1} \tan(\theta_2) + z_{e2} \tan(\theta_1)} \right] \cdot \left[j z_{o1} \frac{z_{o1} \tan(\theta_1) + z_{o2} \tan(\theta_2)}{z_{o1} - z_{o2} \tan(\theta_1) \tan(\theta_2)} \right] = 1$$

$$\text{LHS} = \text{RHS if } z_{e1} z_{o1} = 1 \text{ and } z_{e2} z_{o2} = 1$$

So from equations (4.19) , (4.20),(4.21), (4.22) and (4.26) we get two important conditions

$$z_{e1} z_{o1} = 1 ; z_{e2} z_{o2} = 1 \quad (4.39)$$

From equation (4.19) ,(4.20),(4.21), (4.22) and (4.28) we get

$$\begin{aligned} & k z_{e1}^2 [z_{e2} - z_{e1} \tan(\theta_1) \tan(\theta_2)] [z_{e1} \tan(\theta_1) + z_{o2} \tan(\theta_2)] + \\ & k [z_{e1} \tan(\theta_2) + z_{e2} \tan(\theta_1)] [z_{o2} \tan(\theta_1) - z_{e1}] \\ & = -z_{e1}^2 [1 + \tan^2(\theta_2)] [z_{e2} + z_{o2} \tan^2(\theta_2)] \end{aligned} \quad (4.40)$$

We can solve equations (4.39) and (4.40), when z_{e1} , θ_1 and θ_2 are known.

On solving equations (4.39) and (4.40) and assuming z_{e1} , θ_1 and θ_2 are known, we get following solutions

$$z_{o1} = \frac{1}{z_{e1}} \quad (4.41a)$$

$$z_{e2} =$$

$$\tan(\theta_2) \left[\frac{k \tan^2(\theta_1)(z_{e1}^2 - 1) + \sqrt{k^2 \tan^4(\theta_1)(z_{e1}^2 - 1)^2 - 4z_{e1}^2 [z_{e1}^2 (1 + \tan^2(\theta_1))^2 - k^2 \tan^2(\theta_1)(z_{e1}^2 - 1)^2]}}{2[z_{e1}(1 + \tan^2(\theta_1)) - k \tan(\theta_1)(z_{e1}^2 - 1)]} \right] \quad (4.41b)$$

$$z_{o2} = \frac{k \tan^2(\theta_1)(z_{e1}^2 - 1) - \sqrt{k^2 \tan^4(\theta_1)(z_{e1}^2 - 1)^2 - 4z_{e1}^2 [z_{e1}^2 (1 + \tan^2(\theta_1))^2 - k^2 \tan^2(\theta_1)(z_{e1}^2 - 1)^2]}}{2z_{e1} \tan(\theta_2) [z_{e1}(1 + \tan^2(\theta_1)) - k \tan(\theta_1)(z_{e1}^2 - 1)]} \quad (4.41c)$$

These are the generalized solutions of the proposed coupler.

4.4 Analysis of Circuit Electrical Parameters and Scattering Parameters

Based on the previous theoretical investigation, there are two different kinds of mathematical solutions (Case 1 and Case 2) for this novel coupled-line coupler. How to choose these two cases becomes a serious design problem. For the purpose of explanation, theoretical scattering parameters of typical examples designed using solution (4.35) or (4.41) are presented and discussed. For the convenience of discussion, the coupling coefficients of two-section coupled lines are defined as

$$C_i = \frac{z_{ei} - z_{oi}}{z_{ei} + z_{oi}}, \quad i = 1, 2 \quad (4.42)$$

Case I

For this case the fixed parameters are

$$\theta_1 = 90^\circ, \quad k = 0.95, \quad z_{e1} = 2.05, \quad z_{o1} = 0.8$$

From equation (4.42) we can calculate coupling coefficient for this case

$$C_1 = \frac{2.05 - 0.8}{2.05 + 0.8} = 0.438$$

$$C_1 \text{ (dB)} = -7.17\text{dB}$$

Other parameters such as z_{e2} and z_{o2} can be calculated by using (4.35) when the electrical length varies in the range of 40° to 50° . We can calculate these parameters using MATLAB and plot curves.

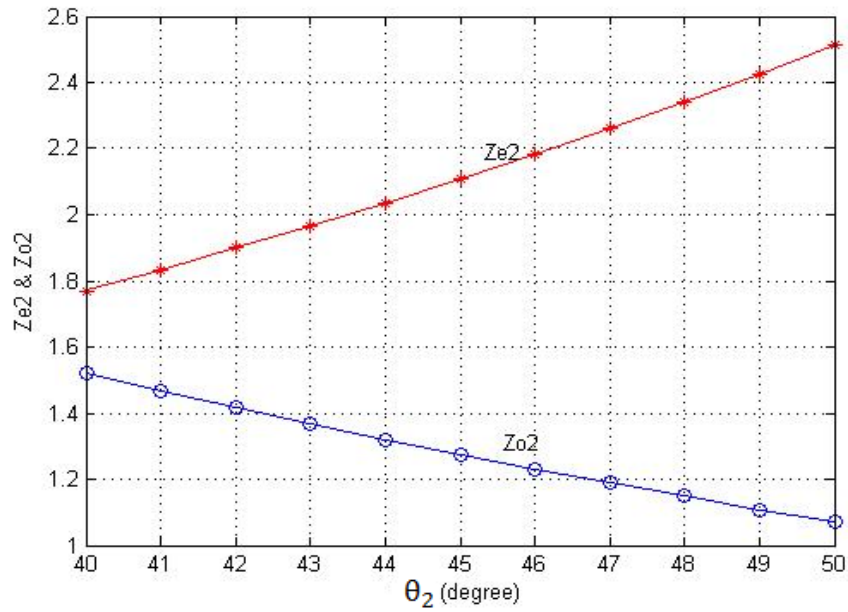


Figure 4.14: Calculated Parameters z_{e2} and z_{o2} with different values of θ_2

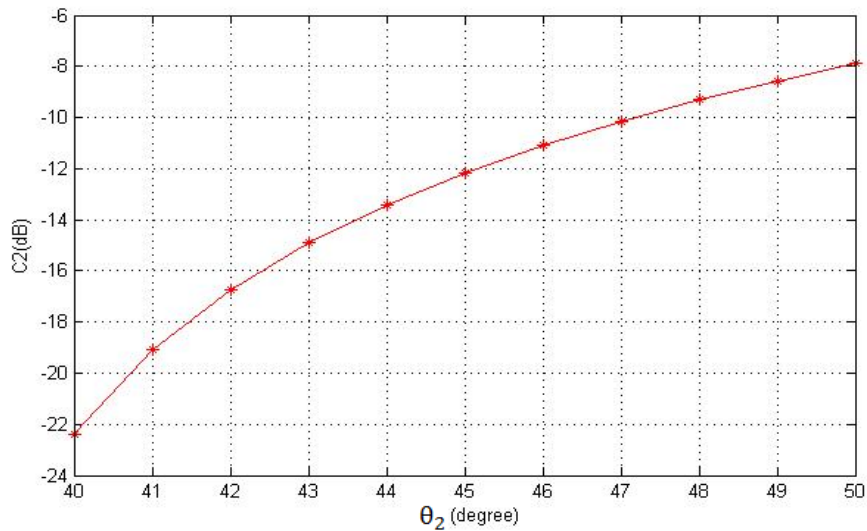


Figure 4.15: Calculated Coupling Coefficient with different values of θ_2

It can be observed from Figure 4.13 and 4.14 that the even-mode (odd-mode) characteristic impedance z_{e2} (z_{o2}) shifts higher (lower) as the electrical length θ_2 increases, indicating a strong coupling for the second section coupled line. The maximum coupling coefficient C_2 of the second coupled-line section is -7.9 dB, thus, two coupled lines have loose coupling.

Therefore, two loosely coupled lines can be used to construct a coupler with external tight coupling performance. According to this numerical analysis, the admissible range of the coupling coefficient of the proposed coupler is $k \geq 0.95$. Although the 40° electrical length θ_2 gives shorter physical length compared to the 50° electrical length θ_2 , the smaller coupling coefficient of the case $\theta_2=40^\circ$ results in a larger separation between coupled lines. Thus, there is a compromise between electrical length and coupling strength.

Theoretical response of the couplers in the normalized frequency band, two typical examples with $\theta_2=40^\circ$ and 50° are shown below.

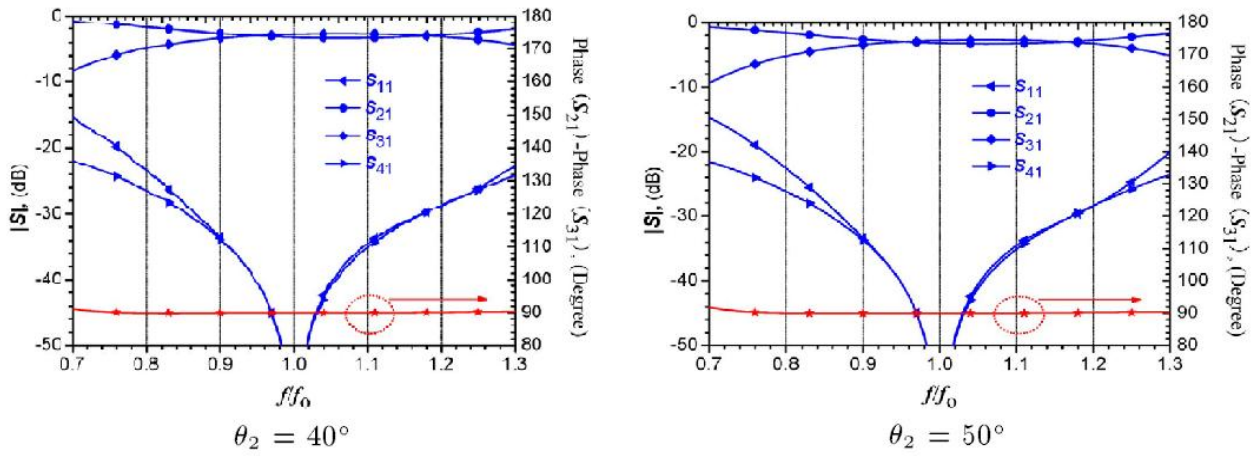


Figure 4.16: Scattering parameters and Phase difference of the coupler with electrical length $\theta_2=40^\circ$ and 50°

Matlab Code for calculated parameters z_{e2}, z_{o2} and Coupling Coefficient are shown in appendix A.

Case II

If the electrical length θ_1 is an arbitrary value in the range of (4.29b), but not equal to 90° , the design equation (4.41) should be chosen.

For this case the fixed parameters are

$$k=3, \theta_2=40^\circ, z_{e1}=1.4$$

From equation (4.41a) we can calculate z_{o1}

$$z_{o1} = \frac{1}{z_{e1}} = \frac{1}{1.4} = 0.7143$$

Other parameters such as z_{e2} and z_{o2} can be calculated by using (4.41) when the electrical length varies in the range of 50° to 60° . We can calculate these parameters using MATLAB and plot curves.

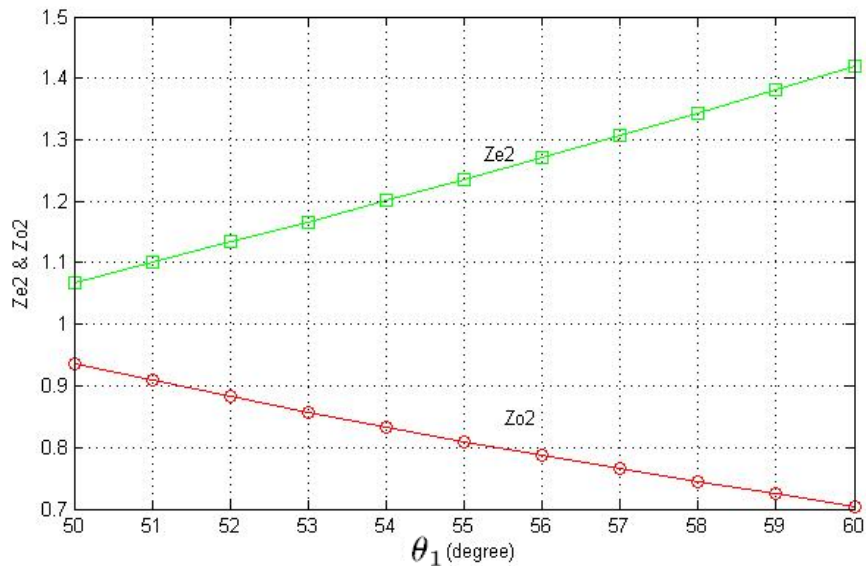


Figure 4.17: Calculated Parameters z_{e2} and z_{o2} with different values of θ_1

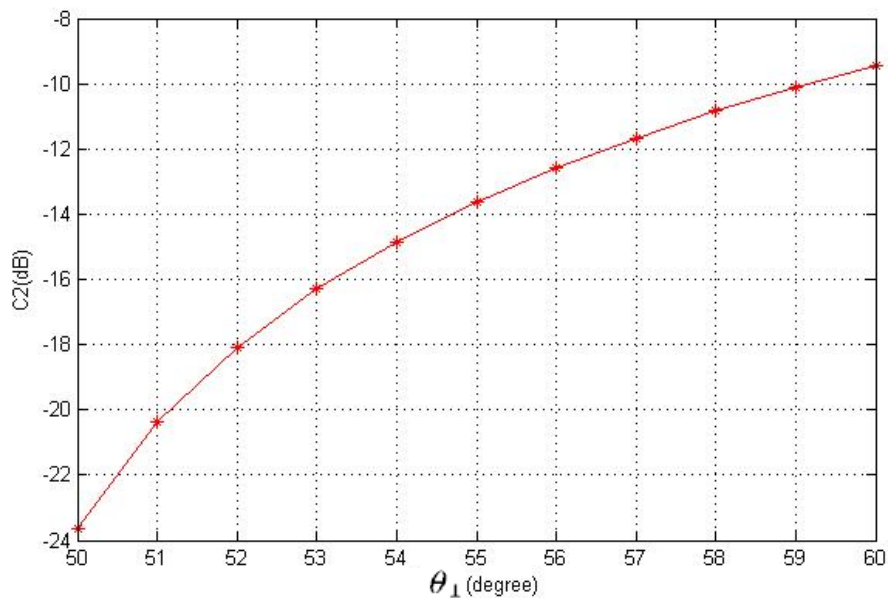


Figure 4.18: Calculated Coupling Coefficient with different values of θ_1

Theoretical response of the couplers in the normalized frequency band, two typical examples with $\theta_1=50^\circ$ and 60° are shown below.

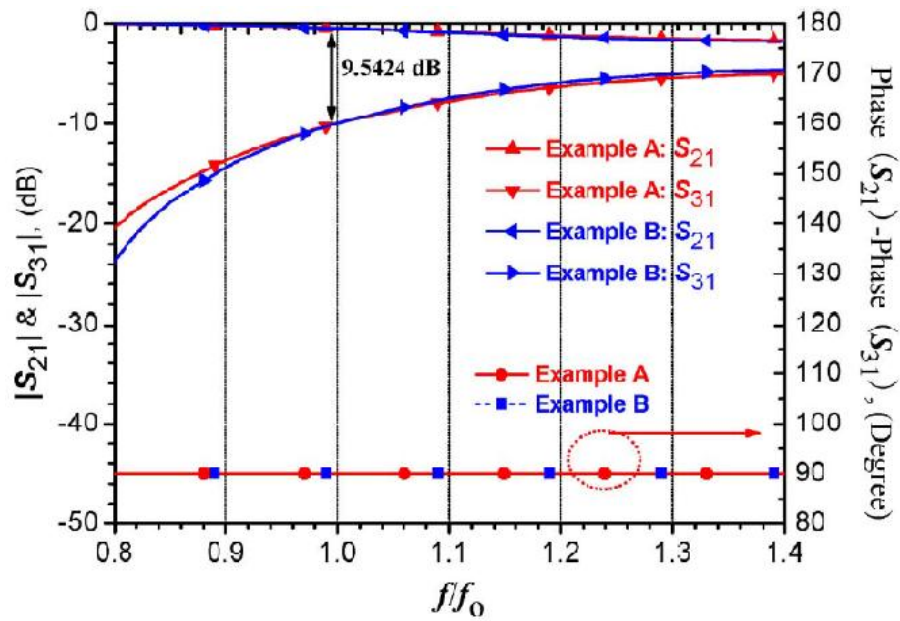


Figure 4.19: Scattering parameters and Phase difference of the coupler with electrical length $\theta_1=50^\circ$ and 60°

Matlab Code for calculated parameters z_{e2}, z_{o2} and Coupling Coefficient are shown in appendix B

CHAPTER 5

SIMULATION AND SIMULATED RESULT

In designing of good coupler some points should be keep in mind. Such as coupler should have good return loss, good impedance match at all ports, high directivity, and strong coupling. Advanced Design System (ADS) 2008 of Agilent is used for designing and simulation of coupler.

5.1 What is Advanced Design System (ADS)?

Advanced Design System is electronic design automation software for RF, microwave, and high speed digital applications. In a powerful and easy-to-use interface, ADS pioneers the most innovative and commercially successful technologies, such as X-parameters and 3D EM simulators, used by leading companies in the wireless communication and networking and aerospace and defence industries [24].

5.2 Full Wave Simulation of Coupler

The design theory and parameter analysis of this proposed coupled-line coupler has been theoretically explained in the previous chapter.

This coupler circuits is designed using an RF substrate with a relatively dielectric constant of 2.65(Benzo-cyclo butane) and a thickness of 2.3 mm. The operating frequency is chosen as 2 GHz. According to design equation (35) based on previously manually chosen parameters such as electrical lengths and port impedance $Z_o = 50\Omega$, the following initial practical electrical parameters are calculated as

$$\theta_1 = 90^\circ, \theta_2 = 48^\circ, k=1$$

$$Z_{e1} = z_{e1} \cdot Z_0 \text{ and } Z_{o1} = z_{o1} \cdot Z_0$$

$$Z_{e1} = 2.05 \times 50 = 102.5\Omega$$

$$Z_{01} = 0.8 \times 50 = 40 \Omega$$

The other parameters Z_{e2} and Z_{o2} can be calculated using equation (35)

$$Z_{e2} = \frac{kz^2_{e1}(z^2_{e1} - z^2_{o1}) + \sqrt{k^2z^4_{e1}(z^2_{e1} - z^2_{o1})^2 - 4z^6_{e1}z^2_{o1}}}{2z^2_{e1} \cot(\theta_2)}$$

$$Z_{o2} = \frac{kz^2_{e1}(z^2_{e1} - z^2_{o1}) - \sqrt{k^2z^4_{e1}(z^2_{e1} - z^2_{o1})^2 - 4z^6_{e1}z^2_{o1}}}{2z^2_{e1} \tan(\theta_2)}$$

On putting the value of θ_2 , k , z_{e1} , z_{o2} in above equation and multiplying Z_0 with we get

$$Z_{e2} = 107.96 \Omega$$

$$Z_{o2} = 62.28 \Omega$$

Now with the help of these parameters we can calculate physical parameters of this coupler. For calculating physical parameters line calculator is used.

ADS Line Calculator

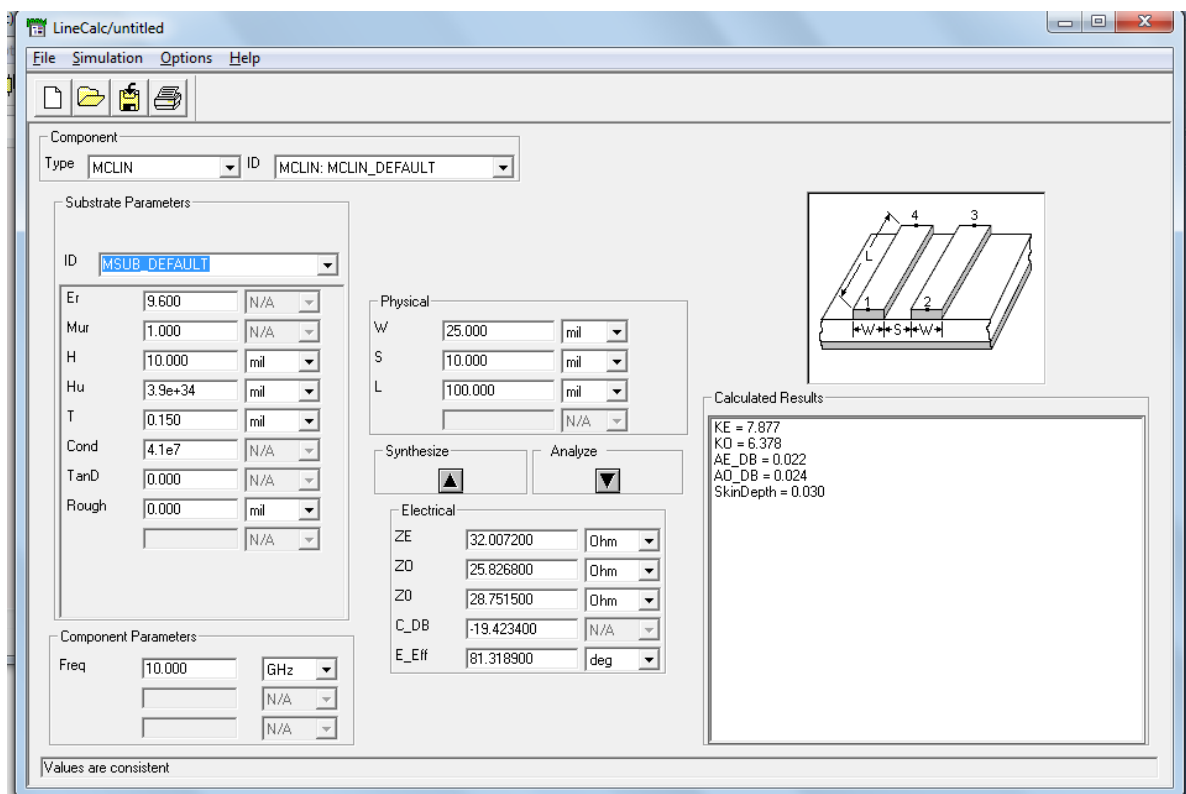


Figure 5.1: ADS Line Calculator

Line Calculator is a tool in Advance Design System (ADS) software by which we can calculate physical parameters from electrical parameters and electrical parameters from physical parameters. The window for line calculator is shown in the figure 5.1.

With the help of Line calculator we can calculate the physical dimensions of both the coupled lines. The initial physical circuit parameters are

$$w_1 = 2.66\text{mm}, s_1 = 0.17\text{mm}, l_1 = 26\text{mm}$$

$$w_2 = 2.05\text{mm}, s_2 = 0.89\text{mm}, l_2 = 14\text{mm}$$

$$w_m = 5.46\text{mm}$$

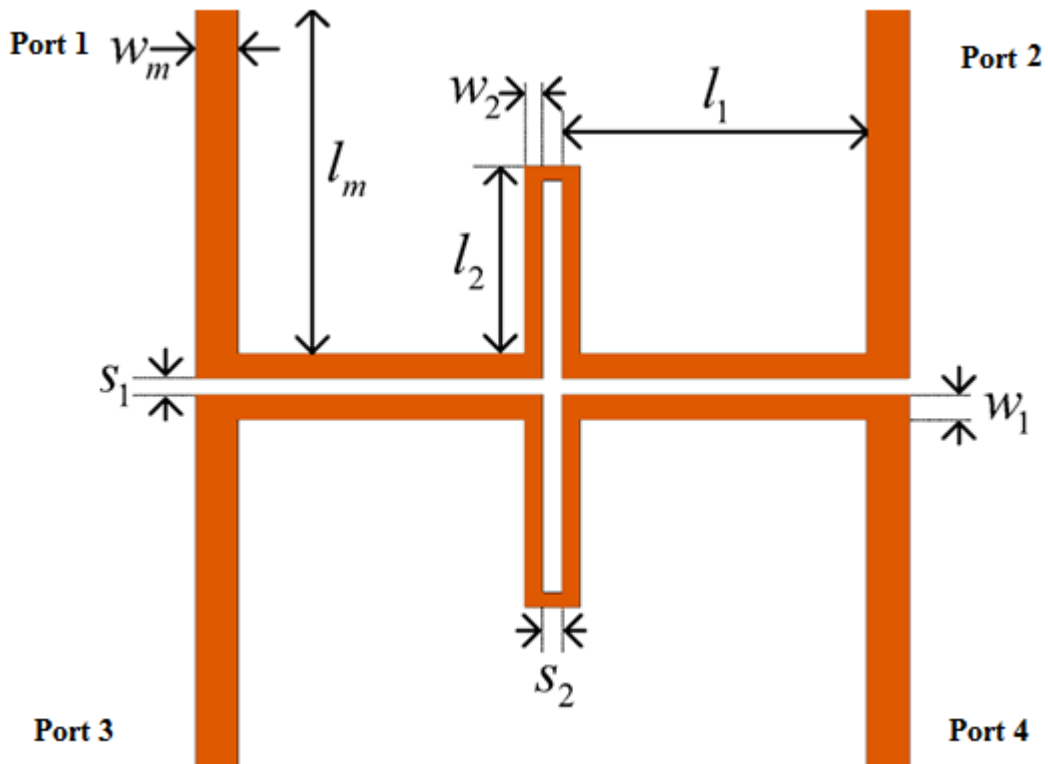


Figure 5.2: Layout of the coupler

Here the length of the port l_m can be chosen according the design requirements. In the figure port 1 is input port, port 2 is through port, port 3 is coupled port and port 4 is isolated port.

The maximum full-wave simulation for the original coupled-line coupler without any optimization is shown below.

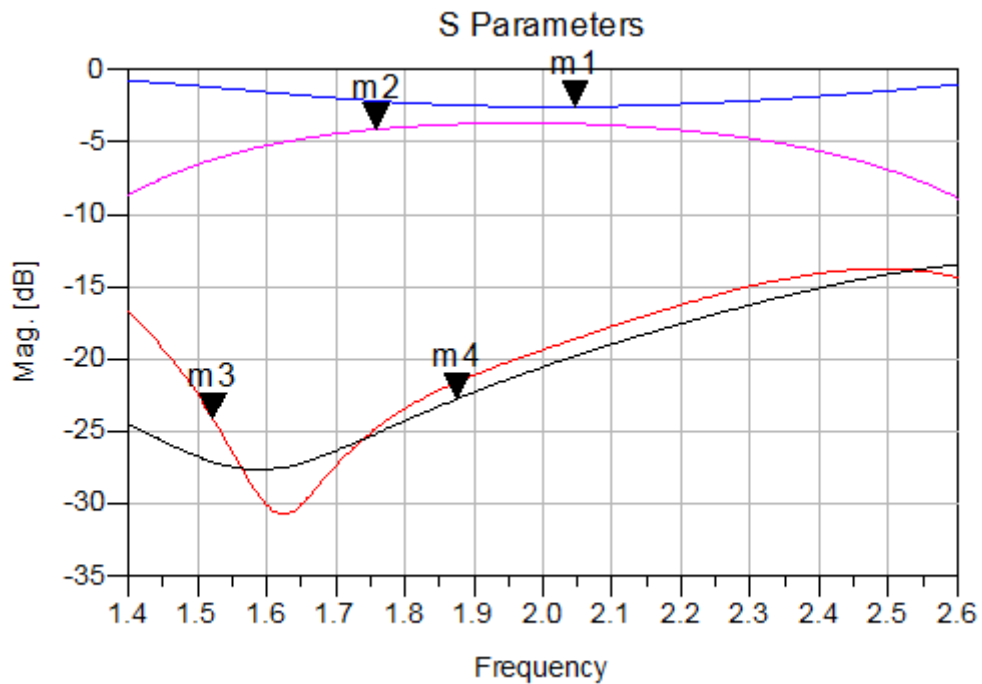


Figure 5.3: Full wave simulated Scattering parameters of Coupler without optimization
m1 is S(2,1),m2 is S(3,1),m3 is S(1,1),m4 is S(4,1)

Here we see that maximum full-wave simulated directivity for the original coupled-line coupler without any optimizations is smaller than 30 dB around 25 dB. So we need to optimize it. Here w_1, w_2, s_1, s_2 are the main parameters which have to be optimized to get high directivity. Here the main parameters are optimized manually.

Optimized Physical Circuit parameters are

$$w_1 = 2.8 \text{ mm}, s_1 = 0.4 \text{ mm}, l_1 = 25 \text{ mm}$$

$$w_2 = 1.8 \text{ mm}, s_2 = 1.0 \text{ mm}, l_2 = 14 \text{ mm}$$

$$w_m = 5.5 \text{ mm}, l_m = 20 \text{ mm}$$

Now we will simulate this circuit using Advance Design System (ADS) Software.

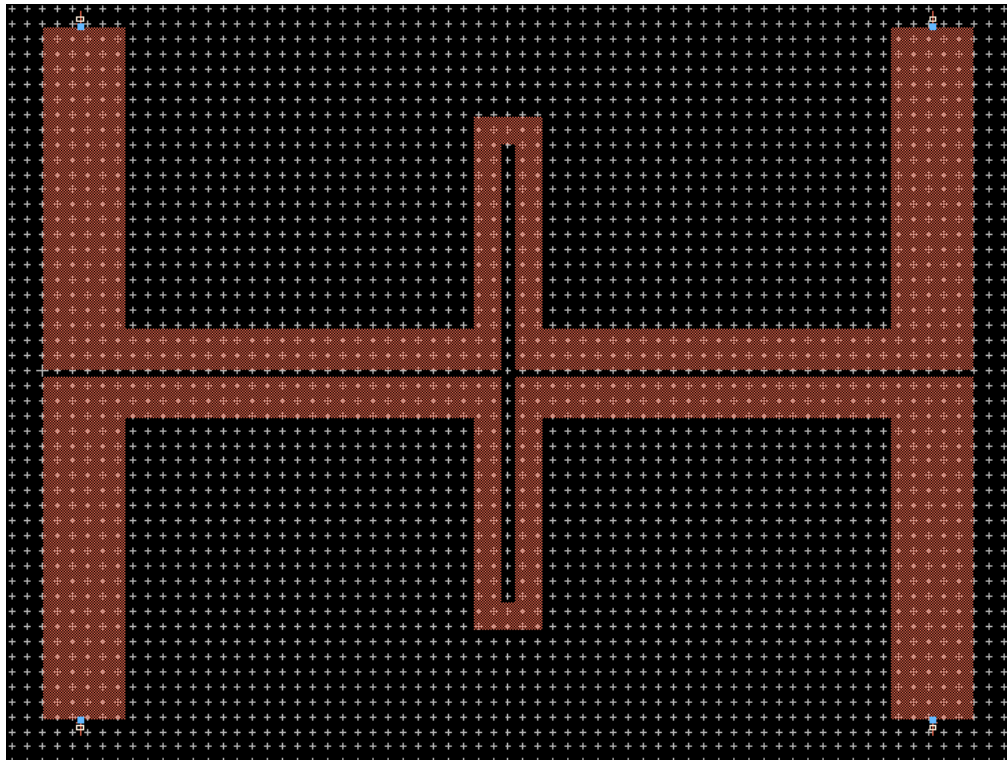


Figure 5.4: Coupler Layout Design in ADS Software

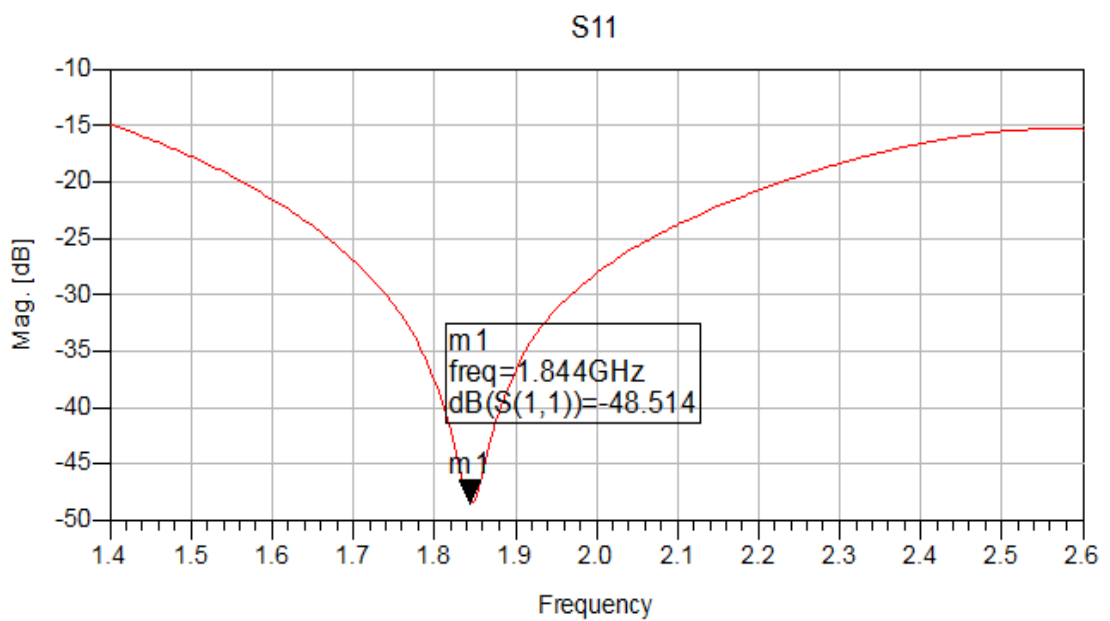


Figure 5.5: Scattering Parameter S11

The above graph shows the reflection from port 1 when signal is applied on the same.

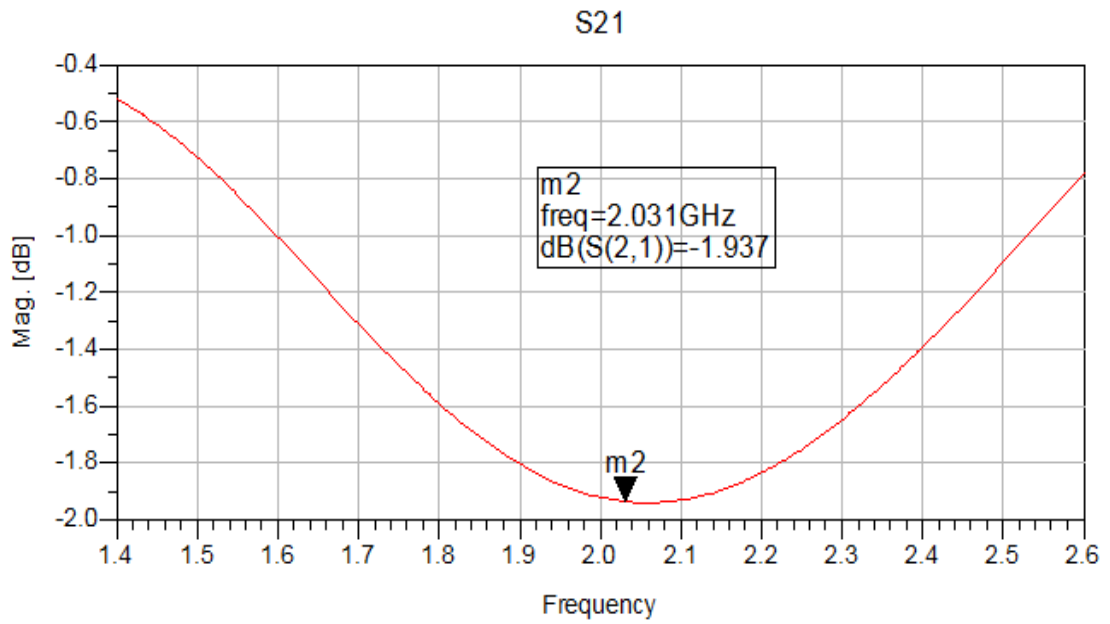


Figure 5.6: Scattering Parameter S21

The above graph shows the output from the port 2 when we apply signal on port 1.

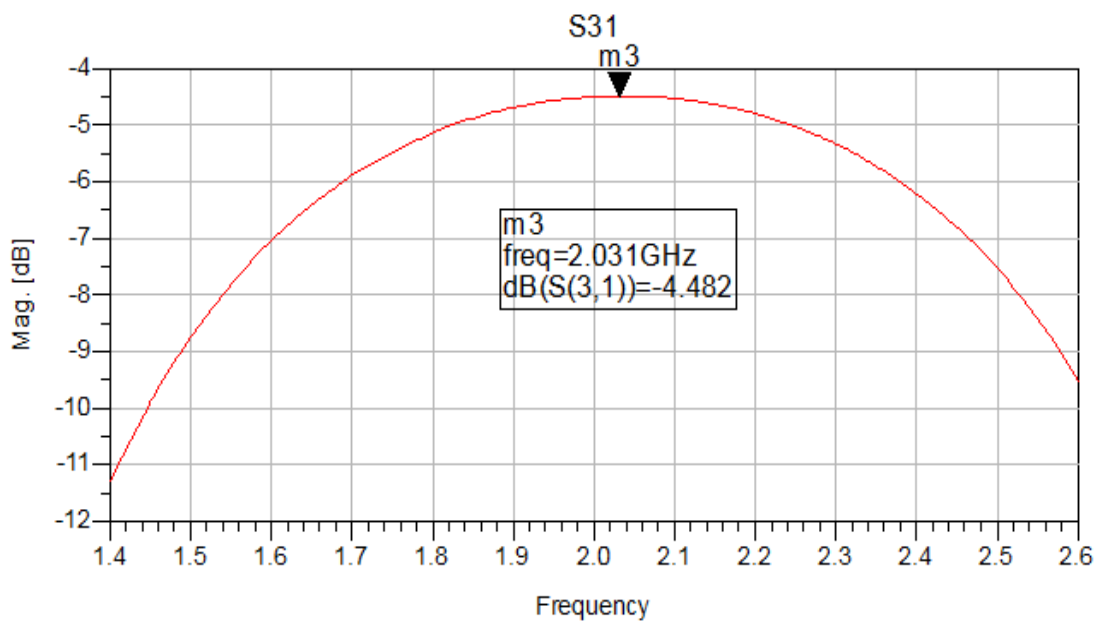


Figure 5.7: Scattering Parameter S31

The above graph shows the output at coupling port or port 3 when signal is applied on the port 1. It shows the maximum coupling -4.482 dB at 2.031 GHz.

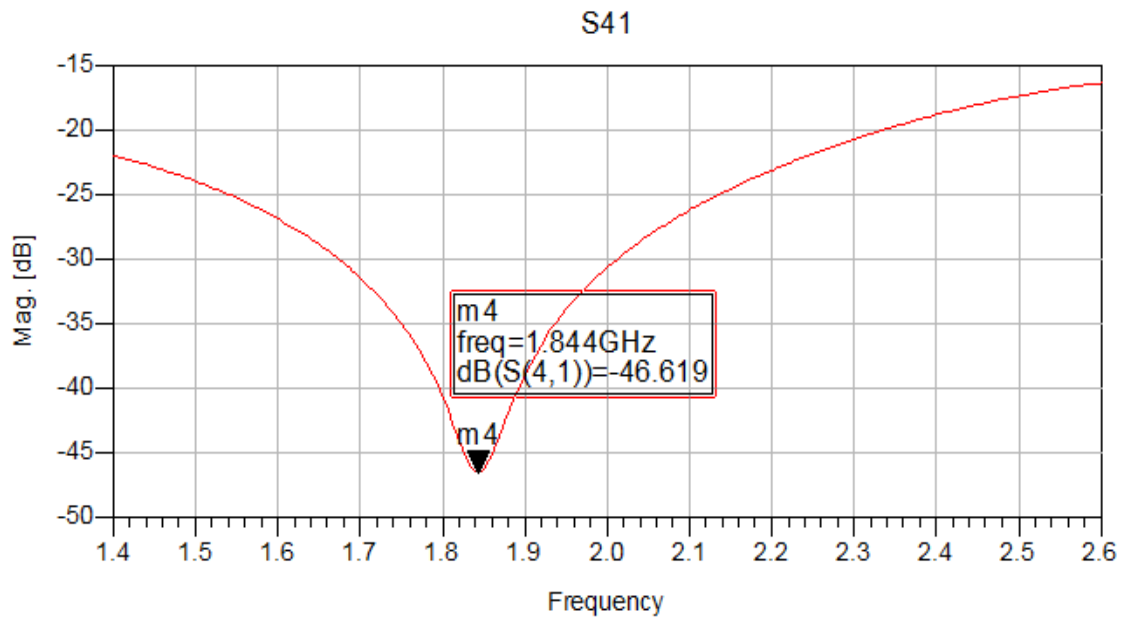


Figure 5.8: Scattering Parameter S41

The above graph shows the output at isolated port or port 4 when we apply signal at port 1. It shows the maximum value -46.619 at 1.844 GHz.

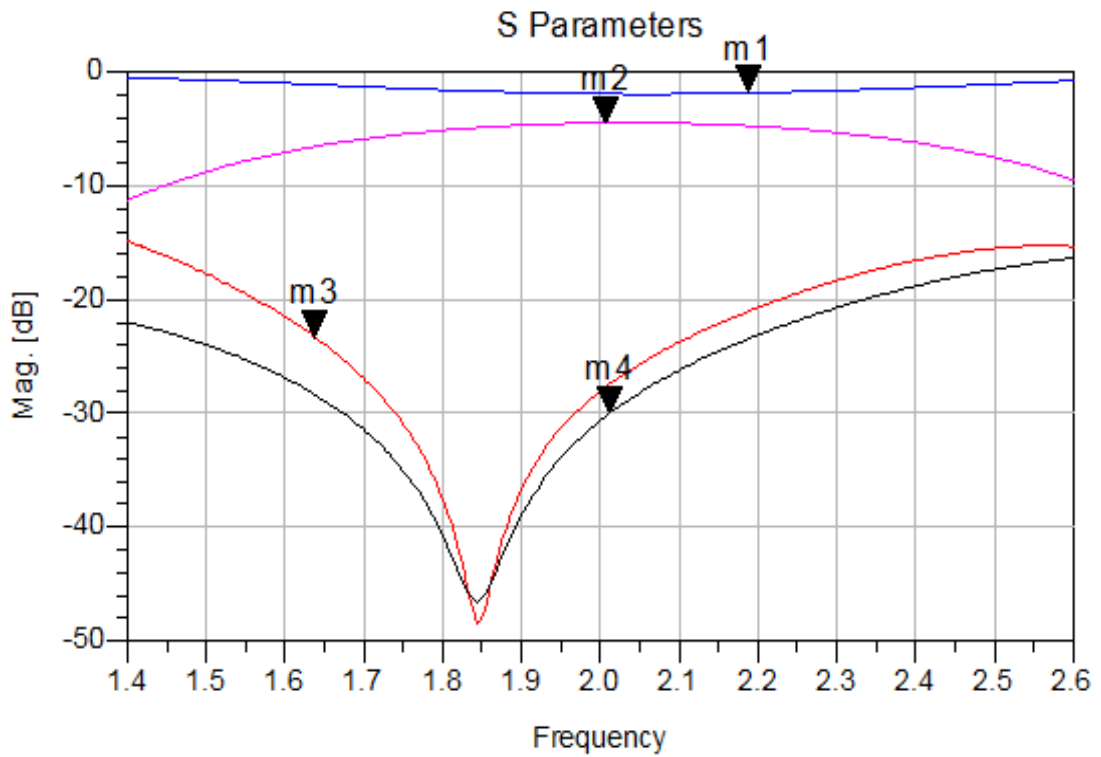


Figure 5.9: Full wave simulated Scattering parameters of Coupler

In the above figure m1 shows the output from port 2 when input signal is applied on port1. m2 shows the output from port 3 when input signal is applied on port1. m4 shows the output from port 4 when input signal is applied on port1.m3 shows the reflection from port 1 when signal is applied on the same port.

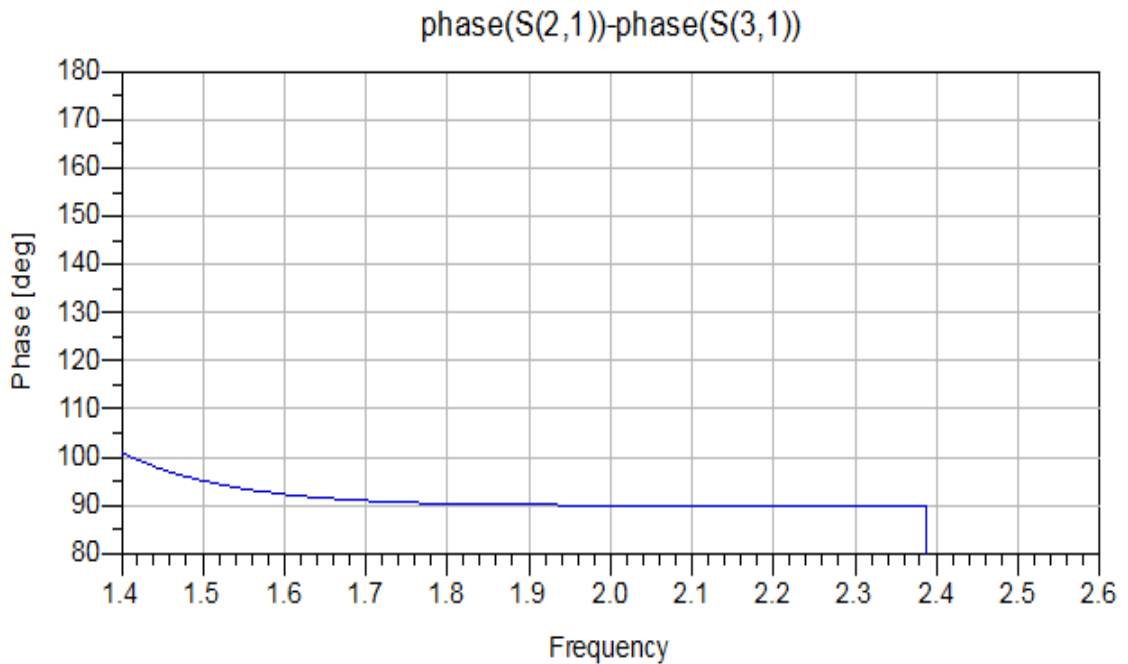


Figure 5.10: Phase difference between S21 and S31

The above figure shows the phase difference between the port 2 and port 3.

5.3 Result

The simulated results are shown from figure 5.5 to 5.10. Figure 5.5 shows that return Loss is 48.514dB at 1.844GHz. Figure 5.6 shows the throughout put of the coupler. Figure 5.7 shows that strongest coupling is 4.482dB at 2.031GHz. Figure 5.8 shows S parameter S41 which is useful for calculation directivity of the coupler.

Highest Directivity is 41.713dB at 1.844GHz. Phase difference is near 90.5 over a wide range from 1.78 to 2.38 GHz.

Results at operating frequency 2GHz are :

Coupling is 4.496 dB

Return loss is 28.074 dB

Directivity is 26.143 dB

The simulated results show that the results after optimization are better than the results without any optimization.

The simulated results of our proposed coupled-line coupler exhibit good return loss, strong coupling, and high directivity. It is very important that this coupler is implemented using common PCB fabrication technology without any limitations.

CHAPTER 6

CONCLUSION AND FUTURE WORK

6.1 Conclusion

In this study a novel coupled-line coupler has been proposed together with the design methodology and full-wave simulation. This coupler, constructed by loose coupled lines, maintains strong coupling and high directivity simultaneously. The simulated return loss, coupling, and directivity are good, which verifies the proposed concept for high-performance couplers. It does not require any extra bonding wires, connectivity through holes, complicated design procedures or multilayer circuitries and large circuit areas.

Due to its simple circuit structure and ease of fabrication and integration in common microstrip systems, this proposed coupler is practical to use, especially in strong coupling situations. The frequency range of this coupler lies in L Band so it can be used in many application of L Band.

Microstrip coupled-line couplers are widely used for the designs of various balanced power amplifiers, mixers, modulators, measurement systems, circularly polarized antennas, beam-forming array antennas, etc.

Coupled line couplers are key components in many wireless communication systems for realizing components such as balanced mixers, balanced amplifiers, power dividers etc.

6.2 Future Work

Due to less time period in this project work it could not possible to do more work but in future, for investigating design of coupler for RF application following work may be extended.

- Since W_1 , W_2 , S_1 and S_2 , are four main controlling parameters. By optimizing these parameters we further can optimize the performance of this coupler i.e. we can increase the directivity and coupling of the coupler.

- By using different type of shape to connect microstrip lines we can develop a coupler which have different frequency band or higher frequency band. For example if we connect two microstrip lines with triangular shape structure then we can shift the frequency band of the coupler to the higher frequency band.

- By changing the dielectric material and its thickness we can further improve the performance of the coupler.

REFERENCES

- [1] R. Mongia, I. Bahl, and P. Bhartia, “RF and Microwave Coupled-Line Circuits”. Boston, MA: Artech House, 1999.
- [2] S. Lee and Y. Lee, “An inductor-loaded microstrip directional coupler for directivity enhancement,” *IEEE Microw. Wireless Compon. Lett.*, vol. 19, no. 6, pp. 362–364, Jun. 2009.
- [3] J. Lange, “Interdigitated strip-line quadrature hybrid,” *IEEE Trans. Microw. Theory Techn.*, vol. MTT-17, no. 12, pp. 1150–1151, Dec. 1969.
- [4] J.-H. Cho, H.-Y. Hwang, and S.-W. Yun, “A design of wideband 3-dB coupler with $\lambda/4$ -section microstrip tandem structure,” *IEEE Microw. Wireless Compon. Lett.*, vol. 15, no. 2, pp. 113–115, Feb. 2005.
- [5] A. M. Abbosh and M. E. Bialkowski, “Design of compact directional couplers for UWB applications,” *IEEE Trans. Microw. Theory Techn.*, vol. 55, no. 2, pp. 189–194, Feb. 2007.
- [6] J.-C. Chiu, C.-M. Lin, and Y.-H. Wang, “A 3-dB quadrature coupler suitable for PCB circuit design,” *IEEE Trans. Microw. Theory Techn.*, vol. 54, no. 9, pp. 3521–3525, Sep. 2006.
- [7] J.-C. Chiu, J.-M. Lin, M.-P. Hwang, and Y.-H. Wang, “A PCB-compatible 3-dB coupler using microstrip-to-CPW via-hole transitions,” *IEEE Microw. Wireless Compon. Lett.*, vol. 16, no. 6, pp. 369–371, Jun. 2006.
- [8] C.-P. Chang, J.-C. Chiu, H.-Y. Chiu, and Y.-H. Wang, “A 3-dB quadrature coupler using broadside-coupled coplanar waveguides,” *IEEE Microw. Wireless Compon. Lett.*, vol. 18, no. 3, pp. 191–193, Mar. 2008.
- [9] Y. X. Guo, Z. Y. Zhang, and L. C. Ong, “Wideband 3-dB coupler using a patterned ground plane,” in Proc. Asia–Pacific Microw. Conf., 2005, vol. 2.

- [10] H.-C. Chen and C.-Y. Chang, "Modified vertically installed planar couplers for ultrabroadband multisection quadrature hybrid," *IEEE Microw. Wireless Compon. Lett.*, vol. 16, no. 8, pp. 446–448, Aug. 2006.
- [11] T. Fujii, I. Ohta, T. Kawai, and Y. Kokubo, "A construction of coupled-line 3-dB couplers using quarter-wave connecting lines," in *Eur. Microw. Conf.*, 2005, vol. 1, pp. 37–40.
- [12] Y.-H. Chun, J.-Y. Moon, S.-W. Yun, and J.-K. Rhee, "Microstrip line directional couplers with high directivity," *Electron. Lett.*, vol. 40, no. 5, pp. 317–318, Mar. 2004.
- [13] K. Wincza and S. Gruszczynski, "Theoretical limits on miniaturization of directional couplers designed as a connection of tightly coupled and uncoupled lines," *Microw. Opt. Technol. Lett.*, vol. 55, no. 1, pp. 223–230, Jan. 2013.
- [14] M.-J. Park and B. Lee, "Compact foldable coupled line cascade couplers," *Proc. Inst. Elect. Eng.—Microw., Antennas, Propag.*, vol. 153, no. 3, pp. 237–240, Jun. 2006.
- [15] J. Muller and A. F. Jacob, "Advanced characterization and design of compensated high directivity quadrature coupler," in *IEEE MTT-S Int. Microw. Symp. Dig.*, 2010, pp. 724–727.
- [16] M. Dydyk, "Microstrip directional couplers with ideal performance via single-element compensation," *IEEE Trans. Microw. Theory Techn.*, vol. 47, no. 6, pp. 956–964, Jun. 1999.
- [17] S. Gruszczynski and K. Wincza, "Generalized methods for the design of quasi-ideal symmetric and asymmetric coupled-line sections and directional couplers," *IEEE Trans. Microw. Theory Techn.*, vol. 59, no. 7, pp. 1709–1718, Jul. 2011.
- [18] I. Ohta, T. Kawai, T. Fujii, and Y. Kokubo, "Directivity improvement of microstrip coupled line couplers based on equivalent admittance approach," in *IEEE MTT-S Int. Microw. Symp. Dig.*, 2003, vol. 1, pp. 43–46.
- [19] S.-F. Chang, J.-L. Chen, Y.-H. Jeng, and C.-T. Wu, "New high-directivity coupler design with coupled spurlines," *IEEE Microw. Wireless Compon. Lett.*, vol. 14, no. 2, pp. 65–67, Feb. 2004.

- [20] R. Islam and G. V. Eleftheriades, "Printed high-directivity metamaterial MS/NRI coupled-line coupler for signal monitoring applications," *IEEE Microw. Wireless Compon. Lett.*, vol. 16, no. 4, pp. 164–166, Apr. 2006.
- [21] David M. Pozra, "Microwave Engineering" 4th ed. Jhone Wiley & Sons, Inc., 2011
- [22] R. E. Collin, *Foundations for Microwave Engineering*, 2nd ed. New York: *IEEE Press*, 1992.
- [23] Yongle Wu, Weinong Sun, Sai-Wing Leung, Yinliang Diao, Kwok-Hung Chan, and Yun-Ming Siu "Single-Layer Microstrip High-Directivity Coupled-Line Coupler With Tight Coupling" *IEEE transaction on Microwave theory and Techniques*, vol.61, no.2, February 2013.
- [24] Advance Design System (ADS) software ver. 2008, by Agilent Technologies.

APPENDIX

A. Matlab Code for calculated parameters z_{e2}, z_{o2} and Coupling Coefficient in case I

Code for z_{e2}, z_{o2}

```
clear all;
close all;
clc;
thita =[40:1:50];
k=.95;
Ze1=2.05;
Zo1=.8;
A=k.*((Ze1).^2);
B=((Ze1).^2)-((Zo1).^2);
C=(4.*((Ze1).^6).*((Zo1).^2));
D=(2.*((Ze1).^2).*(cotd(thita)));
Ze2=((A.*B)+((A.^2).*(B.^2))-C).^^(1/2))./D;
plot(thita,Ze2,'-r*')
gtext('Ze2')
xlabel('thita(degree)')
grid on;
hold on;
E=(2.*((Ze1).^2).*(tand(thita)));
Zo2=((A.*B)-((A.^2).*(B.^2))-C).^^(1/2))./E;
plot(thita,Zo2,'-bo')
gtext('Zo2')
ylabel('Ze2 & Zo2')
grid on;
```

Code for Coupling Coefficient

```
clear all;
close all;
clc;
thita =[40:1:50];
k=.95;
Ze1=2.05;
Zo1=.8;
A=k.*((Ze1).^2);
B=((Ze1).^2)-((Zo1).^2);
C=(4.*((Ze1).^6).*((Zo1).^2));
D=(2.*((Ze1).^2).*(cotd(thita)));
Ze2=((A.*B)+((A.^2).*(B.^2))-C).^^(1/2))./D;
E=(2.*((Ze1).^2).*(tand(thita)));
Zo2=((A.*B)-((A.^2).*(B.^2))-C).^^(1/2))./E;
```

```

c=Ze2-Zo2;
d=Ze2+Zo2;
for i=1:11
K(i)=c(i)/d(i);
end
g=20*log10(K);
plot(thita,g, '-r*')
grid on;
ylabel('C2 (dB)');
xlabel('theta (degree)');

```

B. Matlab Code for calculated parameters z_{e2}, z_{o2} and Coupling Coefficient for case II

Code for z_{e2}, z_{o2}

```

clear all;
close all;
clc;
thital1 =[50:1:60];
k=3;
thita2=40;
Zel=1.4;
Zol=1/Zel;
A=k.*(tand(thital1)).^2;
B=(Zel.^4)-1;
C=2.*Zel;
D=(Zel.*(1+(tand(thital1)).^2));
E=(k.*tand(thital1).*(Zel.^2)-1);
for i=1:11
Ze2(i)=tand(thita2).*((A(i).*B+sqrt(((A(i).*B).^2)-(C.^2).*(D(i).^2)-(E(i).^2))))/(C.*(D(i)+E(i))));
end
plot(thital1,Ze2, '-gs')
gtext('Ze2')
xlabel('thita (degree)')
grid on;
hold on;
for i=1:11
Zo2(i)=(A(i).*B-sqrt(((A(i).*B).^2)-(C.^2).*(D(i).^2)-(E(i).^2))))/(tand(thita2).*(C.*(D(i)-E(i))));
end
plot(thital1,Zo2, '-ro')
gtext('Zo2')
ylabel('Ze2 & Zo2')
grid on;

```

Code for Coupling Coefficient

```
clear all;
close all;
clc;
thital = [50:1:60];
k=3;
thita2=40;
Zel=1.4;
Zo1=1/Zel;
A=k.*(tand(thital)).^2;
B=(Zel.^4)-1;
C=2.*Zel;
D=(Zel.*(1+(tand(thital)).^2));
E=(k.*tand(thital).*((Zel.^2)-1));
for i=1:11
Ze2(i)=tand(thita2).*(A(i).*B+sqrt(((A(i).*B).^2)-
(C.^2).*((D(i).^2)-(E(i).^2))))/(C.*(D(i)+E(i)));
end

for i=1:11
Zo2(i)=(A(i).*B-sqrt(((A(i).*B).^2)-(C.^2).*((D(i).^2)-
(E(i).^2))))/(tand(thita2).*(C.*(D(i)-E(i))));
end
c=Ze2-Zo2;
d=Ze2+Zo2;
for i=1:11
K(i)=c(i)/d(i);
end
g=20*log10(K);
plot(thital,g,'-r*')
grid on;
ylabel('C2 (dB)');
xlabel('thetal (degree)');
```